Published OnlineFirst August 14, 2014; DOI: 10.1158/1078-0432.CCR-14-0742

After incubation, responder CD4 or CD8 T cells (1×10^5) harvested from the stimulation culture were washed and then pulsed with 17 16-mer OLPs for CD4 T cells or 35 12-mer OLPs for CD8 T cells with GolgiStop monensin (Sigma Chemical Co.) for 3 hours. After incubation, cytokine production by CD4 and CD8 T cells was detected by intracellular cytokine staining (ICS).

Intracellular cytokine staining

The cells harvested from culture were washed and stained with anti-CD3-PerCP/Cy5.5 (clone SK7; eBioscience) and anti-CD4-V500 (BD Horizon), or anti-CD3-APC/Cy7 (clone HIT3a; BioLegend), anti-CD8-V500 (clone RPA-T8; BD Horizon), and anti-CD107a-FITC (clone H4A3; BD Pharmingen; 2 μL) for 30 minutes on ice. After incubation, the cells were washed, fixed, and permeabilized with Cytofix/Cytoperm solution (Pharmingen, Becton Dickinson) for 20 minutes at 4°C. Then, the cells were washed in Perm/Wash solution (Pharmingen), and pelleted cells were stained for intracellular cytokines using anti-IFNγ-PE/Cy7 (clone 4S.B3; eBioscience), anti-TNFα-PE/Cy7 (clone MAb11; eBioscience), anti-IL-5-PE (clone JES1-39D10; BD Horizon), anti-IL-13-PE (clone JES10-5A2; BD Horizon), anti-IL-17A-Brilliant Violet 421 (clone BL168; BioLegend), anti-IL-17F-V450 (clone O33-782; BD Pharmingen), and anti-IL-10-APC (clone JES3-19F1; BioLegend) for detection of CD4 cytokines or anti-IFNγ-PerCP/Cy5.5 (clone 4S.B3; eBioscience), anti-TNFα-Brilliant Violet 421 (clone MAb11; BioLegend), and anti-IL-10-APC (clone JES3-19F1; BioLegend) for detection of CD8 cytokines for 30 minutes on ice. After incubation, the cells were washed and analyzed by FACS Canto II (BD Bioscience). The data were analyzed using FlowJo software (version 7.6.5; Tree Star). If the number of cytokine-staining cells stimulated with XAGE1 (GAGED2a) OLPs was more than 2-fold the number of staining cells stimulated with control peptides, it was defined as positive (23).

Overall survival

The diagnosis of lung cancer was done pathologically within a month after the first visit. OS was measured from the day of diagnosis and analyzed by the Kaplan–Meier method. Differences in survival between patient subgroups were analyzed using the log-rank test. Univariate and multivariate analyses using Cox proportional hazards regression model were performed to assess the association of each factor with OS. *P* values less than 0.05 were considered significant.

Statistical analysis

Statistical analysis was performed with the Student *t* test for two groups and with ANOVA for multiple groups using IBM SPSS Statistics 19 for Windows (IBM). Quantitative data without a normal distribution were analyzed with nonparametric tests, and data with a normal distribution were analyzed with parametric tests. For a two-sample comparison of continuous variables, Wilcoxon rank-sum test was performed. For analysis of the correlation of the extrapolated titer and each parameter, Pearson rank test was performed. Results are expressed as the mean or 95% confidence interval (95% CI).

Results

XAGE1 (GAGED2a) antibody response in patients with advanced lung adenocarcinoma

Characteristics of 145 patients with advanced (clinical stage IIIB and IV) lung adenocarcinoma investigated in this study are shown in Supplementary Table S1A. We evaluated the serum IgG response against XAGE1 (GAGED2a) in the patients by ELISA using a synthetic protein. An extrapolated titer was calculated for each serially diluted serum sample as described (24). The IgG response was defined as positive for sera with extrapolated titers exceeding or equal to 100. Thirty-three patients were antibody positive and titration curves of sera are shown in Fig. 1A. The dominant IgG subtypes were IgG1 and IgG3, and no IgG2 or IgG4 response was observed (Fig. 1B). The positive response was further classified by extrapolated titers as $+++ \geq 6{,}400$, $6{,}400 > ++ \geq 1{,}600$, $1{,}600 > + \geq 400$, and $400 >$ weak ≥ 100 (Fig. 1C).

A higher antibody response frequency was observed in patients with EGFRmt tumors than in patients with EGFRwt tumors of the 145 patients (Supplementary Table S1A). However, no significant difference was observed for the antibody response in any characteristics in 58 patients with XAGE1 (GAGED2a) antigen-positive tumors (data not shown).

Detection of CD4 and CD8 T-cell responses in PBMCs from XAGE1 (GAGED2a) antibody-positive advanced lung adenocarcinoma patients

Purified CD4 and CD8 T cells in PBMCs from XAGE1 (GAGED2a) antibody-positive advanced lung adenocarcinoma patients were stimulated for 12 days with CD4- and CD8-depleted PBMCs treated with XAGE1 (GAGED2a) 17 16-mer OLPs or a synthetic protein, respectively. After culture, the cells were collected and cytokine production was examined for CD4 T cells after 3-hour stimulation with XAGE1 (GAGED2a) 17 16-mer OLPs and for CD8 T cells after 3-hour stimulation with XAGE1 (GAGED2a) 35 12-mer OLPs by ICS. As shown in Fig. 1D and Supplementary Fig. S1, IFNγ/TNFα, IL5/IL13, and IL17A/IL17F-producing CD4 T cells were detected in PBMCs from 7, 1, and 3 of 11 patients examined, respectively. IL10-producing CD4 T cells were not detected in any of the patients. On the other hand, IFNγ- and TNFα-producing CD8 T cells were detected in PBMCs from 4 and 6 of 11 patients, respectively. IL10-producing CD8 T cells were not detected in any. No XAGE1 (GAGED2a) antibody responses or CD4 or CD8 T-cell responses were detected in healthy individuals as reported previously (21).

Phenotypic analyses of CD4 T cells and MDSCs in PBMCs from XAGE1 (GAGED2a) antibody-positive patients

Th1, Th2, Th17, and T_{FH} CD4 T cells, resting and activated CD4 Tregs (25), and M- and PMN-MDSCs in PBMCs from XAGE1 (GAGED2a) antibody-positive patients were analyzed by flow cytometry (Supplementary Fig. S2). As

Published OnlineFirst August 14, 2014; DOI: 10.1158/1078-0432.CCR-14-0742

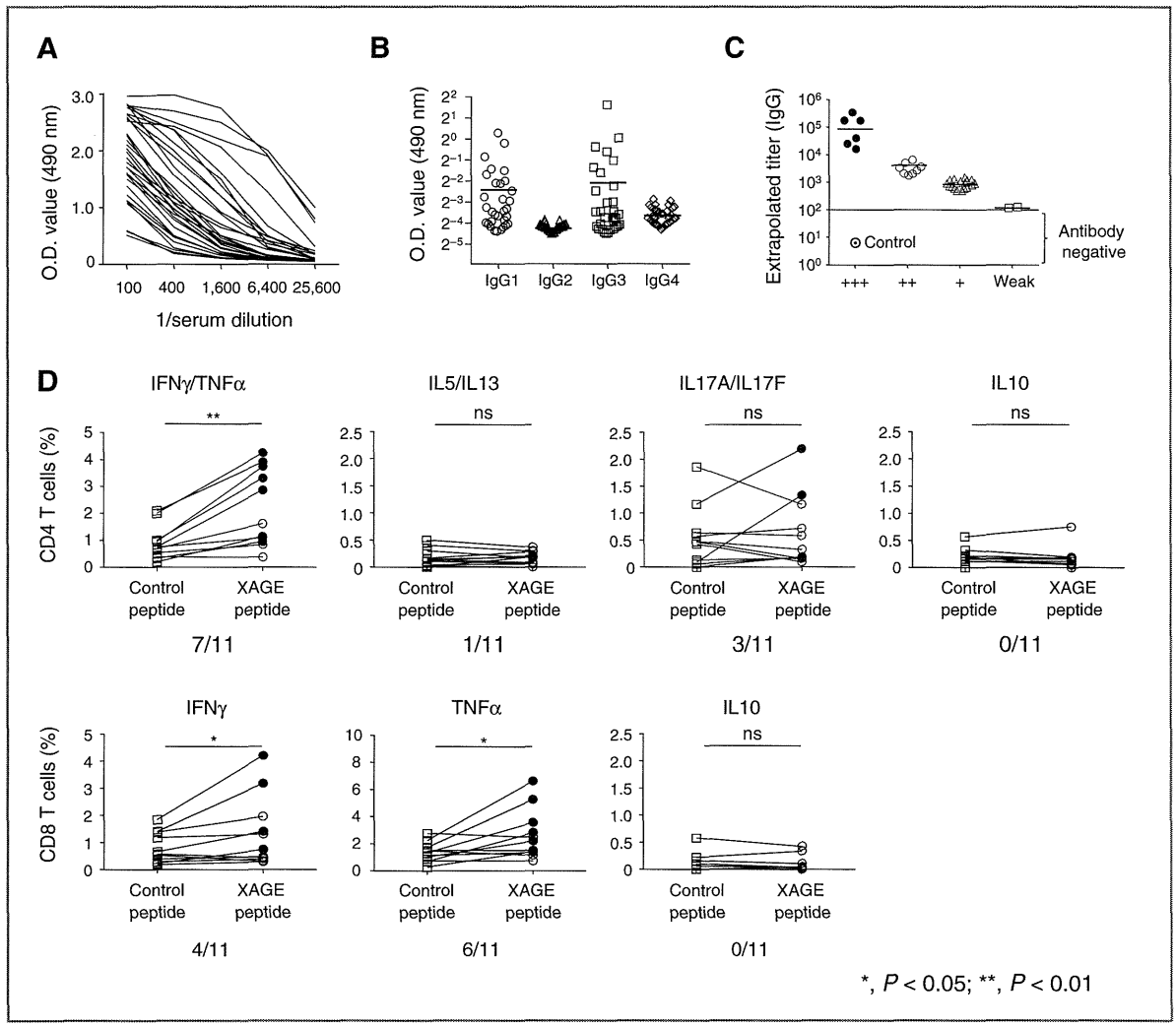

Figure 1. Antibody and T-cell responses against XAGE1 (GAGED2a) in patients with advanced lung adenocarcinoma. A, titration curves of positive sera from 33 of 145 patients investigated. ELISA was done using synthetic XAGE1 (GAGED2a) protein. The IgG response was defined as positive for sera with an extrapolated titer exceeding or equal to 100. B, serum IgG subtypes reactive to synthetic XAGE1 (GAGED2a) protein determined by ELISA with diluted sera (1:100) using a subtype-specific antibody. C, classification of positive responses against XAGE1 (GAGED2a) by an extrapolated titer as $+++ \geq 6{,}400, 6{,}400 > ++ \geq 1{,}600, 1{,}600 > + \geq 400$, and $400 >$ weak ≥ 100. D, CD4 and CD8 T cells (1×10^6) purified from PBMCs of XAGE1 (GAGED2a) antibody-positive patients were cultured with an equal number of irradiated (40 Gy), autologous CD4-, and CD8-depleted PBMCs as APCs in the presence of XAGE1 (GAGED2a) 17 16-mer OLPs (10^{-6} mol/L) or the synthetic protein (10^{-6} mol/L), respectively, using 48-well culture plates for 12 days. The cells were then collected and cytokine production was examined for CD4 T cells after 3-hour stimulation with XAGE1 (GAGED2a) 17 16-mer OLPs and for CD8 T cells after 3-hour stimulation with XAGE1 (GAGED2a) 35 12-mer OLPs by intracellular cytokine staining (ICS). Control peptides (a mixture of MGARASVLSGGELDR and ASVLSGGELDRWEKI) were from Con B gag motifs of the human immunodeficiency virus. Cytokine-staining cells stimulated with XAGE1 (GAGED2a) OLPs at more than 2-fold the number of staining cells stimulated with control peptides was defined as positive (filled circles). The number of positive patients out of 11 patients investigated is shown in each panel. Statistical analysis was done by the Wilcoxon rank test (*, $P < 0.05$; **, $P < 0.01$). Each line indicates a single patient.

shown in Fig. 2A, all Th1, Th2, Th17, and T_{FH} CD4 T-cell levels were elevated in XAGE1 (GAGED2a) antibody-positive patients compared with those in antibody-negative patients. A decrease in activated, but not resting, Treg levels was also observed (Fig. 2B). Furthermore, a decrease in the M-MDSC level and an increase in the PMN-MDSC level were observed (Fig. 2C). Th1, Th2, and Th17/total Treg and Th1, Th2, and Th17/total MDSC levels were increased (Fig. 2D and E). An increase in T_{FH}/total MDSC, but not the T_{FH}/Treg level, was observed (Fig. 2D and E).

Analysis of CD4 and CD8 T cells expressing T-cell activation and inhibitory molecules in PBMCs from XAGE1 (GAGED2a) antibody-positive patients

CD4 and CD8 T cells expressing T-cell activation molecules ICOS, OX40, 4-1BB, and GITR, and T-cell inhibitory

Published OnlineFirst August 14, 2014; DOI: 10.1158/1078-0432.CCR-14-0742

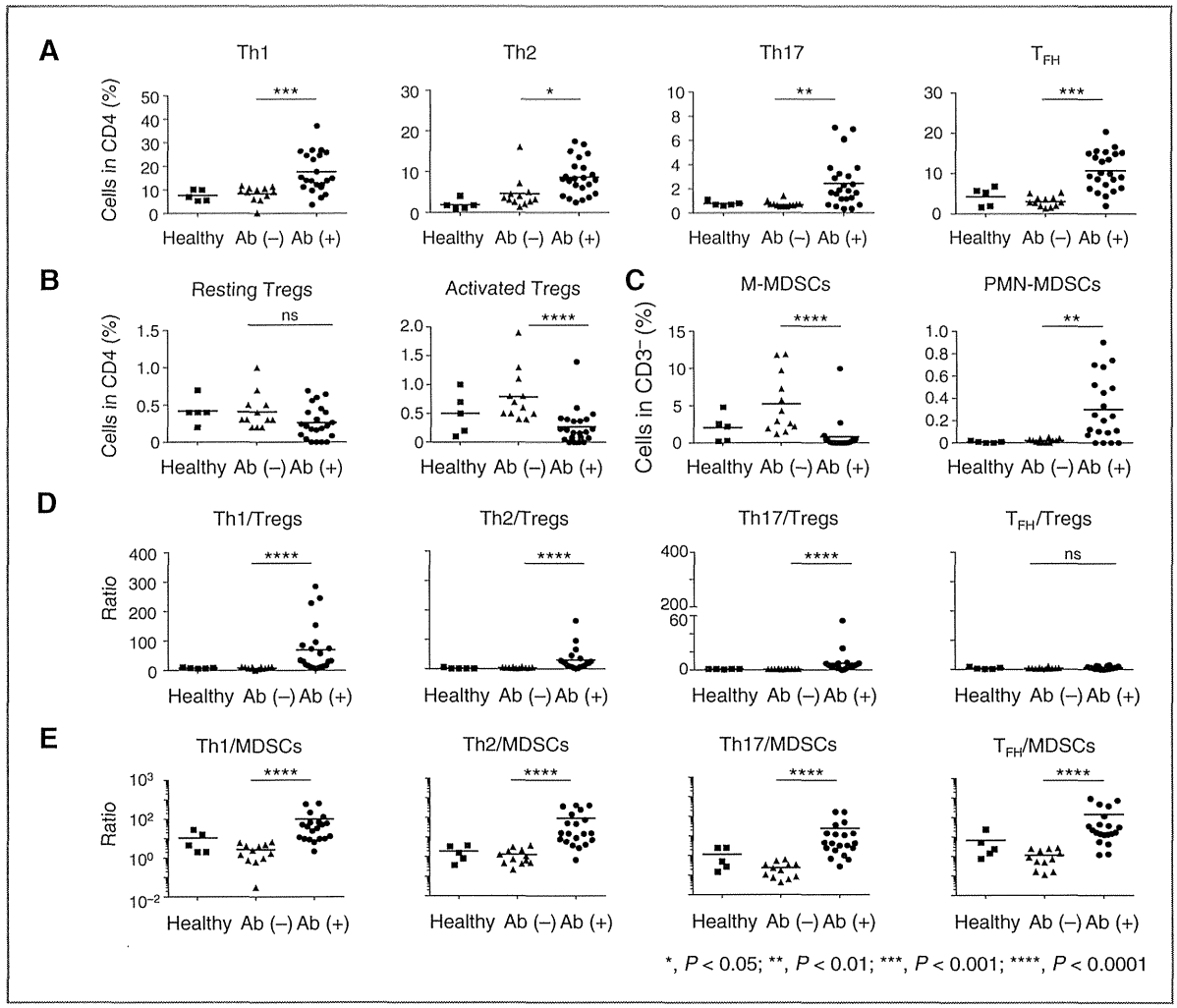

Figure 2. Phenotypic analyses of CD4 T cells (A and B) and MDSCs (C) in PBMCs from 23 XAGE1 (GAGED2a) antibody-positive and 12 negative patients, and 5 healthy donors by FACS. D and E show the ratio of each phenotype of T cells to Tregs and MDSCs, respectively. Statistical analysis was done by the Student *t* test for two groups and by ANOVA for multiple groups (*, $P < 0.05$; **, $P < 0.01$; ***, $P < 0.001$; ****, $P < 0.0001$). Each dot indicates a single patient.

molecules 2B4, BTLA, PD-1, and Tim-3 in PBMCs from XAGE1 (GAGED2a) antibody-positive patients were investigated. As shown in Fig. 3 and Supplementary Fig. S3, an increase in ICOS and PD-1–positive cell levels and a decrease in BTLA-positive cell levels were observed in CD4 T cells from antibody-positive patients compared with those in CD4 T cells from antibody-negative patients. On the other hand, a decrease in GITR-positive cell levels was observed in CD8 T cells from antibody-positive patients.

Overall survival of XAGE1 (GAGED2a) antibody-positive and -negative patients

The OS of XAGE1 (GAGED2a) antibody-positive and -negative patients was analyzed for 145 patients with advanced lung adenocarcinoma. Patient characteristics are shown in Supplementary Table S1A, as described above.

OS was first analyzed for the patients with XAGE1 (GAGED2a) antigen-positive and -negative tumors. As shown in Fig. 4A, no significant difference was found in OS between them ($P = 0.22$, HR, 0.78). However, prolongation of OS was observed in XAGE1 (GAGED2a) antibody-positive patients compared with antibody-negative patients ($P = 0.006$, HR, 0.53; Fig. 4B). The median OS times in the antibody-positive and -negative patients were 33.3 months and 15.1 months, respectively. Antibody-negative patients were then stratified by the XAGE1 (GAGED2a) antigen expression in the tumor. As shown in Fig. 4C, the antibody-negative patients with antigen-positive tumors showed shortened survival. The median

Published OnlineFirst August 14, 2014; DOI: 10.1158/1078-0432.CCR-14-0742

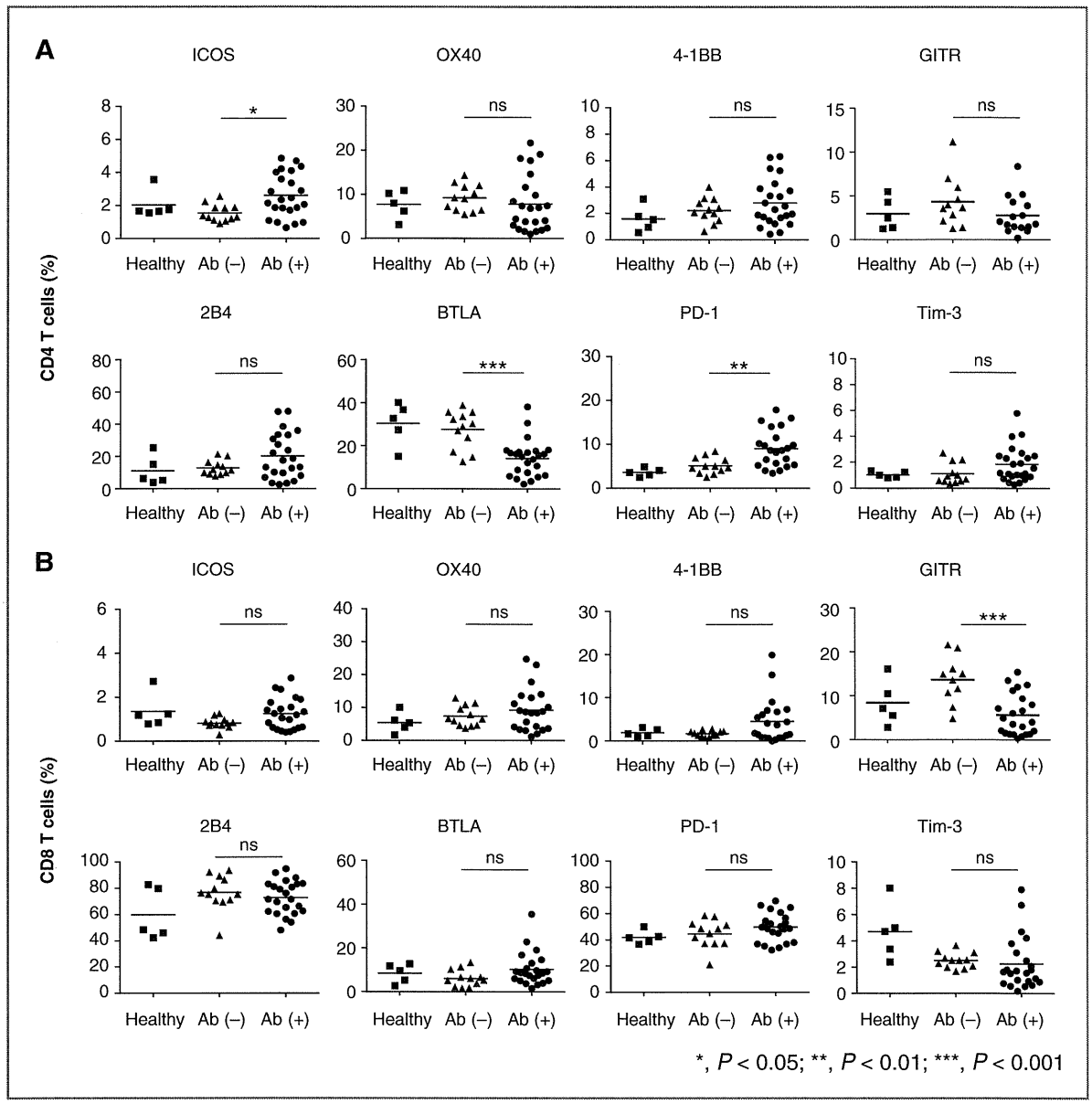

Figure 3. Analysis of CD4 (A) and CD8 (B) T cells expressing T-cell activation (ICOS, OX40, 4-1BB, and GITR) and inhibitory (2B4, BTLA, PD-1, and Tim-3) molecules in PBMCs from XAGE1 (GAGED2a) antibody-positive and negative patients, and healthy donors by FACS. Statistical analysis was done by the Student *t* test for two groups and by ANOVA for multiple groups (*, $P < 0.05$; **, $P < 0.01$; ***, $P < 0.001$). Each dot indicates a single patient.

OS in the patients with antigen-positive tumors was 33.3 months when antibody-positive, but only 13.7 months when antibody-negative ($P < 0.0001$, HR, 0.34). Furthermore, prolongation of OS was dependent on the IgG titer (Supplementary Fig. S4).

The patients were further stratified by the absence or presence of the EGFR mutation in the tumor. The patients with EGFRmt tumors treated with EGFR-TKI and conventional platinum-based doublet chemotherapy showed prolonged OS compared with the patients with EGFRwt tumors treated with conventional chemotherapy alone ($P = 0.017$; Fig. 5A and C and Supplementary Fig. S5A). OS was prolonged by the presence of antibodies in patients with XAGE1 (GAGED2a) antigen-positive EGFRwt or EGFRmt tumors (Fig. 5B and D). The median OS in the patients with XAGE1 (GAGED2a) antigen-positive EGFRwt tumors was 31.5 months when antibody-positive, but only 15.6 months when antibody-negative ($P = 0.05$, HR, 0.46; Fig. 5B). On the other hand, in the patients with XAGE1 (GAGED2a) antigen-positive EGFRmt tumors, the median OS was 34.7

Published OnlineFirst August 14, 2014; DOI: 10.1158/1078-0432.CCR-14-0742

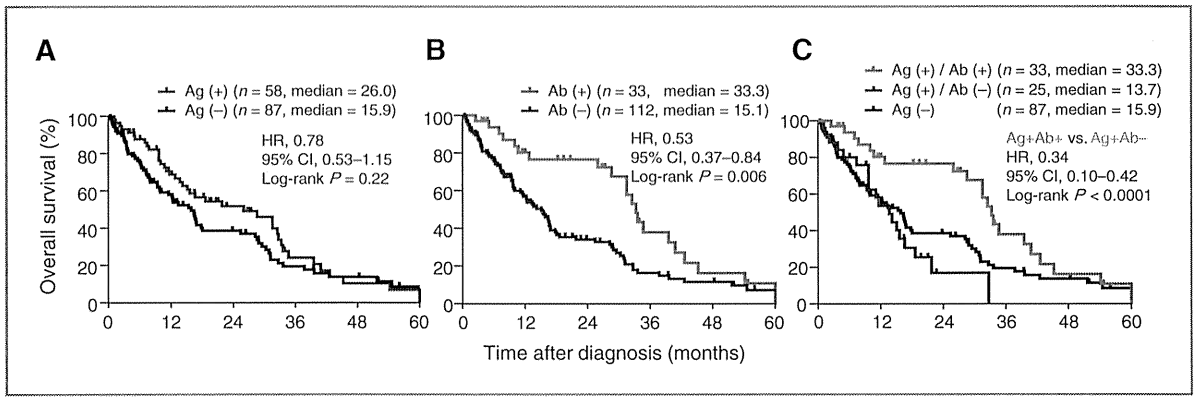

Figure 4. OS of patients with advanced lung adenocarcinoma with XAGE1 (GAGED2a) antigen-expressing or nonexpressing tumors (A), with and without the XAGE1 (GAGED2a) antibody (B), and with the antigen expressing or nonexpressing tumors and with or without the antibody (C).

months when antibody-positive, but only 11.1 months when antibody-negative ($P = 0.001$, HR, 0.28; Fig. 5D). No significant difference was found in OS in the antibody-positive patients with EGFRwt and EGFRmt tumors, or the patients with antigen-negative EGFRmt tumors ($P = 0.36$; Fig. 5B and D and Supplementary Fig. S5B).

OS of patients with different EGFR mutation tumors

EGFR mutation types were defined in 44 tumors (Supplementary Table S1B). Mutations in exon 18 (G719A/C/S), exon 19 (E746-A750 deletion: type 1, E746-A750 deletion: type 2 and L747-P753 deletion and S insertion), and exon 21 (L858R and L861Q) were detected. As shown in Supplementary Fig. S6, no significant difference in OS was observed in patients with different EGFR mutation tumors ($P = 0.44$).

Univariate and multivariate analyses

We performed univariate and multivariate analyses on OS in 145 patients with advanced lung adenocarcinoma. Univariate analysis showed that the presence of the XAGE1 (GAGED2a) antibody, EGFR mutation, good Eastern Cooperative Oncology Group performance status, or never or light smoking habit were significant predictors for prolonged OS (Supplementary Table S2A). On the other hand, multivariate analysis showed that the presence of the XAGE1 (GAGED2a) antibody was a strong predictor for prolonged OS in patients with XAGE1 (GAGED2a) antigen-positive tumors ($P < 0.0001$, HR, 0.18) and in patients with either EGFRwt ($P = 0.04$, HR, 0.50) or EGFRmt tumors ($P = 0.002$, HR, 0.17; Supplementary Table S2B). XAGE1 (GAGED2a) antigen expression was a worse predictor in patients with EGFRmt tumors ($P = 0.004$, HR, 5.23).

Augmented or sustained antibody response, but increased immune inhibition, during the late phase of disease progression

The XAGE1 (GAGED2a) antibody response was examined for a prolonged period until death by disease progression in 13 XAGE1 (GAGED2a) antigen-positive advanced lung adenocarcinoma patients. The numbers of antibody-positive and -negative patients were 10 and 3, respectively. As shown in Fig. 6A, antibody response was augmented in 5 of 10 antibody-positive patients and sustained in 5 other patients. No positive conversion was observed in 3 antibody-negative patients. With 5 antibody response-augmented patients, various immune parameters were compared at diagnosis and at the late phase of disease progression. As shown in Fig. 6B, an increase in $CXCR5^+$ (T_{FH}) CD4 T-cell level, but not $CXCR3^+$ (Th1) CD4 T-cell level, was observed. No change in resting or activated Treg levels was observed (Fig. 6C). M- and PMN-MDSC levels were increased at the late phase (Fig. 6C). An increase in Tim-3 expression level was observed in CD8 T cells (Fig. 6D). Functional analysis showed that impaired XAGE1 (GAGED2a)-specific CD4 (Fig. 6E) and CD8 (Fig. 6F) T-cell responses for cytokine production were observed frequently at the late phase.

Discussion

In this study, we demonstrated that XAGE1 (GAGED2a) antibody-positive advanced lung adenocarcinoma patients showed prolonged OS when compared with the OS of antibody-negative patients. In patients with XAGE1 (GAGED2a) antigen-positive tumors, no significant difference was found in OS in patients with EGFRwt and EGFRmt tumors when they were XAGE1 (GAGED2a) antibody-positive (Fig. 5 and Supplementary Fig. S5). It should be noted that the patients with EGFRmt tumors treated with EGFR-TKI and conventional platinum-based doublet chemotherapy showed prolonged OS compared with those with EGFRwt tumors treated with conventional chemotherapy alone (Supplementary Fig. S5). The presence of the antibody greatly prolonged OS in patients with XAGE1 (GAGED2a) antigen-positive EGFRwt tumors, resulting in OS close to that of antibody-positive patients with EGFRmt tumors.

The patients with XAGE1 (GAGED2a) antigen-positive EGFRmt tumors showed shortened OS when the patients were antibody-negative compared with that of those with

Published OnlineFirst August 14, 2014; DOI: 10.1158/1078-0432.CCR-14-0742

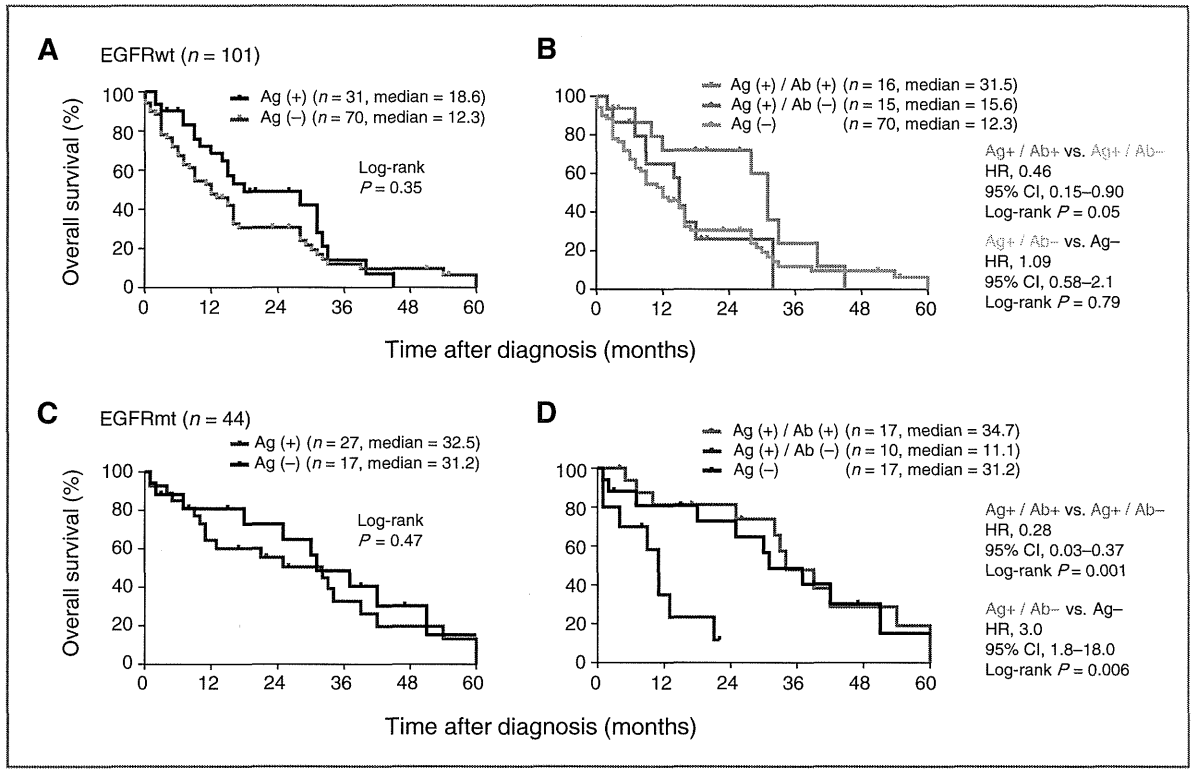

Figure 5. OS of the patients with advanced lung adenocarcinoma with XAGE1 (GAGED2a) antigen-expressing or nonexpressing EGFRwt (A and B) and EGFRmt (C and D) tumors and with or without the antibody (B and D).

antigen-negative EGFRmt tumors. It should be noted that the survival shortening effect of XAGE1 (GAGED2a) antigen expression was observed only in patients with EGFRmt tumors, but not in those with EGFRwt tumors. These findings suggest specific involvement of the XAGE1 (GAGED2a) antigen in EGFRmt tumors or with EGFR-TKI treatment. The presence of the XAGE1 (GAGED2a) antigen in a tumor may facilitate EGFR-mediated tumorigenesis and/or hamper the effect of EGFR-TKI, and the presence of the XAGE1 (GAGED2a) antibody may inhibit this effect. EGFR signaling was delivered via the PI3K, AKT, and mTOR, or Ras, Raf, MEK, and MAPK pathways to activate many tumorigenic genes (26–30). These involve cell cycle, cell proliferation, antiapoptosis, invasion, or metastasis (31–33). Although the XAGE1 (GAGED2a) antigen has been shown to locate in the nucleus, the possibility of direct molecular interaction between XAGE1 (GAGED2a) and mutated EGFR, its downstream molecules, or EGFR-TKI itself remains to be addressed.

The function of the XAGE1 (GAGED2a) molecule is largely unknown. However, Caballero and colleagues (34) recently showed that *XAGE1* depletion in an SK-MEL-37 melanoma cell line by siRNAs reduced proliferation, clonogenic survival, migration, and invasion of the cells. The tumorigenic effect of cancer/testis antigen on the X chromosome (CT-X) was also shown in *SSX4* (34) and *MAGE* (35, 36). For *XAGE*-related *GAGE* genes, the proteins bind to the metazoan transcriptional regulator, germ cell-less (GCL), at the nuclear envelope and cause tumorigenesis (37). These findings suggest that the tumorigenic effect is a common characteristic of CT-X antigens.

CT-X expression has been shown to be a marker of poor outcome in non–small cell lung cancer (NSCLC) (38). The expressions of NY-ESO-1, MAGE-A1, MAGE-A3, and SSX2 were associated with shorter survival in lung adenocarcinoma. Especially, high-level expression of NY-ESO-1 or MAGE was a strong predictor for worse outcome independent of confounding factors such as stage, histology, and therapy. With XAGE1 (GAGED2a), no significant difference was observed in OS with the antigen-positive and negative-patients. Moreover, we previously reported that no correlation was found between the expression pattern (diffuse, intermediate, or focal) and OS (19). It is possible that the higher frequency of antibody response causing prolonged survival may obscure the difference.

The prolongation of OS by the presence of the XAGE1 (GAGED2a) antibody counteracting the survival shortening effect of XAGE1 (GAGED2a) antigen expression may not result from direct interaction of the antibody and antigen. The XAGE1 (GAGED2a) antigen resides in the cells, usually in the nucleus as mentioned above. It is unlikely that the antibody enters the cell and interacts with XAGE1

Published OnlineFirst August 14, 2014; DOI: 10.1158/1078-0432.CCR-14-0742

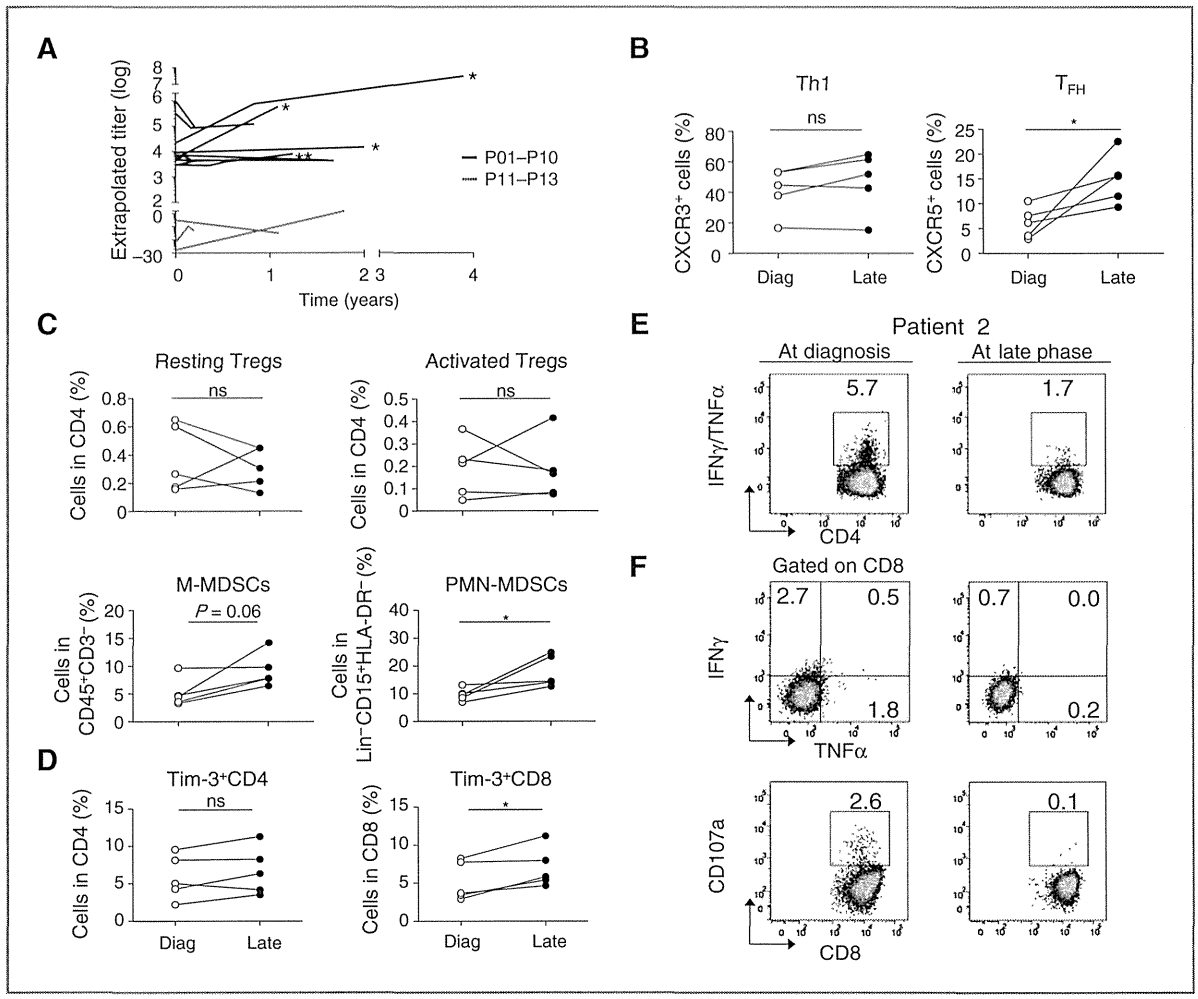

Figure 6. Augmented or sustained antibody response, but increased immune inhibition, during the late phase of disease progression in XAGE1 (GAGED2a) antigen-positive, advanced lung adenocarcinoma patients. A, kinetic XAGE1 (GAGED2a) antibody response by ELISA during a prolonged period until death by disease progression in 10 XAGE1 (GAGED2a) antibody-positive (P01–P10, black lines) and 3 antibody-negative (P11–P13, red lines) patients. Five patients showing an increase in antibody titer are denoted by asterisks and were analyzed for CXCR3 and CXCR5-positive CD4 T cells (B), resting and activated Tregs, and M- and PMN-MDSCs (C), and Tim-3 expression in CD4 and CD8 T cells (D) at diagnosis or at the late phase by FACS. Statistical analysis was done by the Wilcoxon rank test (*, $P < 0.05$). Each line indicates a single patient. E and F show the responses of CD4 and CD8 T cells, respectively, against the XAGE1 (GAGED2a) antigen determined for cytokine production by ICS as described in the Fig. 1D legend. In F, the expression of the CD107a molecule on CD8 T cells was also analyzed by FACS.

(GAGED2a). Rather, it is likely that T-cell responses elicited concomitantly with the antibody response contribute to the antitumor effect. Our previous (21) and present results showed frequent occurrence of CD4 and CD8 T-cell responses in XAGE1 (GAGED2a) antibody-positive patients and no such T-cell responses in antibody-negative patients. Thus, CD4 and CD8 T-cell responses seemed to be associated with the antibody response in patients with XAGE1 (GAGED2a)-positive tumors. In patients with NY-ESO-1–positive tumors, such a naturally occurring integrated immune response was frequently observed (39, 40). NY-ESO-1 is a prototype of the CT antigen and has been shown to be strongly antigenic (41). XAGE1 (GAGED2a) seemed to be less immunogenic than NY-ESO-1 (21), but still capable of eliciting an integrated immune response. In our previous study, we demonstrated that XAGE1 (GAGED2a) expression resulted in shorter survival in patients with NSCLC when the MHC class I expression was downregulated in the tumor (20). However, when the tumor coexpressed XAGE1 (GAGED2a) and MHC class I, survival was clearly prolonged. These findings suggest the involvement of CD8 T-cell activation in recognizing the XAGE1 (GAGED2a) antigen on HLA class I may contribute to prolonged survival.

On the other hand, recent exome analysis to determine mutations in the tumor has revealed the relevance of

Published OnlineFirst August 14, 2014; DOI: 10.1158/1078-0432.CCR-14-0742

immune responses to multiple mutated gene products in the tumor (42–45). Because XAGE1 (GAGED2a) expression is mostly heterogeneous, the immune response to XAGE1 (GAGED2a) could be a surrogate for such immune responses to mutated antigens.

In this study, we characterized various immune parameters in XAGE1 (GAGED2a) antibody-positive patients and showed elevated immune responsiveness. XAGE1 (GAGED2a)-reactive CD4 and CD8 T cells were detected in the antibody-positive patients. Increases in Th1, 2, 17, T_{FH} levels and decreases in activated Treg and M-MDSC levels were observed in the antibody-positive patients. An increase in ICOS and PD-1–expressing CD4 T-cell levels and a decrease in BTLA-expressing CD4 T-cell levels were observed in the antibody-positive patients. These findings suggested that in XAGE1 (GAGED2a) antibody-positive patients, immune activation involving CD4 and CD8 T cells occurred in response to the XAGE1 (GAGED2a) antigen, supporting elicitation of an integrated immune response.

At the late phase of disease progression long after finishing treatment, the XAGE1 (GAGED2a) antibody response was still augmented or sustained. $CXCR3^+$ (Th1) and $CXCR5^+$ (T_{FH}) CD4 T-cell levels were retained or increased. However, increases in M- and PMN-MDSC, and Tim-3–expressing CD8 T-cell levels were observed. A reduction in XAGE1 (GAGED2a)-reactive CD4 and CD8 T-cell responses was frequently observed at the late phase. These findings suggest that immune regulation is one of the causes leading to disease progression resulting in death, even in patients with prolonged survival.

Disclosure of Potential Conflicts of Interest

No potential conflicts of interest were disclosed.

Authors' Contributions

Conception and design: Y. Ohue, Y. Mizote, M. Oka, E. Nakayama
Development of methodology: Y. Ohue, Y. Mizote
Acquisition of data (provided animals, acquired and managed patients, provided facilities, etc.): Y. Ohue, K. Kurose, M. Fukuda, M. Oka
Analysis and interpretation of data (e.g., statistical analysis, biostatistics, computational analysis): Y. Ohue, Y. Mizote, M. Oka, E. Nakayama
Writing, review, and/or revision of the manuscript: Y. Ohue, M. Oka, E. Nakayama
Administrative, technical, or material support (i.e., reporting or organizing data, constructing databases): Y. Ohue, H. Matsumoto, Y. Nishio, M. Isobe, M. Fukuda, A. Uenaka, M. Oka
Study supervision: M. Oka, E. Nakayama

Acknowledgments

The authors thank Junko Mizuuchi for the preparation of the article.

Grant Support

This work was supported in part by a grant from Cancer Research Institute, N.Y., by JSPS KAKENHI (23591169 and 26830117), by a grant from the Okayama Medical Foundation, by a grant from Kawasaki Medical School, and by a grant from Kawasaki University of Medical Welfare. This study was performed as a research program of the Project for Development of Innovative Research on Cancer Therapeutics (P-DIRECT), Ministry of Education, Culture, Sports, Science and Technology of Japan.

The costs of publication of this article were defrayed in part by the payment of page charges. This article must therefore be hereby marked *advertisement* in accordance with 18 U.S.C. Section 1734 solely to indicate this fact.

Received March 26, 2014; revised June 26, 2014; accepted July 14, 2014; published OnlineFirst August 14, 2014.

References

1. Old LJ, Chen YT. New paths in human cancer serology. J Exp Med 1998;187:1163–7.
2. Simpson AJ, Caballero OL, Jungbluth A, Chen YT, Old LJ. Cancer/testis antigens, gametogenesis and cancer. Nat Rev Cancer 2005;5:615–25.
3. Hofmann O, Caballero OL, Stevenson BJ, Chen YT, Cohen T, Chua R, et al. Genome-wide analysis of cancer/testis gene expression. Proc Natl Acad Sci U S A 2008;105:20422–7.
4. CT database. Available from: http://www.cta.lncc.br. Accessed February 15, 2014.
5. Rosenberg SA. A new era for cancer immunotherapy based on the genes that encode cancer antigens. Immunity 1999;10:281–7.
6. Scanlan MJ, Gure AO, Jungbluth AA, Old LJ, Chen YT. Cancer/testis antigens: an expanding family of targets for cancer immunotherapy. Immunol Rev 2002;188:22–32.
7. Old LJ. Cancer vaccines: an overview. Cancer Immun 2008;8 Suppl 1:1.
8. Caballero OL, Chen YT. Cancer/testis (CT) antigens: potential targets for immunotherapy. Cancer Sci 2009;100:2014–21.
9. Brinkmann U, Vasmatzis G, Lee B, Pastan I. Novel genes in the PAGE and GAGE family of tumor antigens found by homology walking in the dbEST database. Cancer Res 1999;59:1445–8.
10. Brinkmann U, Vasmatzis G, Lee B, Yerushalmi N, Essand M, Pastan I. PAGE-1, an X chromosome-linked GAGE-like gene that is expressed in normal and neoplastic prostate, testis, and uterus. Proc Natl Acad Sci U S A 1998;95:10757–62.
11. Liu XF, Helman LJ, Yeung C, Bera TK, Lee B, Pastan I. XAGE-1, a new gene that is frequently expressed in Ewing's sarcoma. Cancer Res 2000;60:4752–5.
12. Vega Genome Browser. Available from: http://vega.sanger.ac.uk/Homo_sapiens/Location/Overview/region?db=core;g=OTTHUMG00000021557;r=X:52057788–52857787. Accessed February 15, 2014.
13. Wang T, Fan L, Watanabe Y, McNeill P, Fanger GR, Persing DH, et al. L552S, an alternatively spliced isoform of XAGE-1, is over-expressed in lung adenocarcinoma. Oncogene 2001;20:7699–709.
14. Egland KA, Kumar V, Duray P, Pastan I. Characterization of overlapping XAGE-1 transcripts encoding a cancer testis antigen expressed in lung, breast, and other types of cancers. Mol Cancer Ther 2002;1:441–50.
15. Zendman AJ, van Kraats AA, den Hollander AI, Weidle UH, Ruiter DJ, van Muijen GN. Characterization of XAGE-1b, a short major transcript of cancer/testis-associated gene XAGE-1, induced in melanoma metastasis. Int J Cancer 2002;97:195–204.
16. Zendman AJ, Van Kraats AA, Weidle UH, Ruiter DJ, Van Muijen GN. The XAGE family of cancer/testis-associated genes: alignment and expression profile in normal tissues, melanoma lesions and Ewing's sarcoma. Int J Cancer 2002;99:361–9.
17. Sato S, Noguchi Y, Ohara N, Uenaka A, Shimono M, Nakagawa K, et al. Identification of XAGE-1 isoforms: predominant expression of XAGE-1b in testis and tumors. Cancer Immun 2007;7:5.
18. Ali Eldib AM, Ono T, Shimono M, Kaneko M, Nakagawa K, Tanaka R, et al. Immunoscreening of a cDNA library from a lung cancer cell line using autologous patient serum: Identification of XAGE-1b as a dominant antigen and its immunogenicity in lung adenocarcinoma. Int J Cancer 2004;108:558–63.
19. Nakagawa K, Noguchi Y, Uenaka A, Sato S, Okumura H, Tanaka M, et al. XAGE-1 expression in non-small cell lung cancer and antibody response in patients. Clin Cancer Res 2005;11:5496–503.

Published OnlineFirst August 14, 2014; DOI: 10.1158/1078-0432.CCR-14-0742

20. Kikuchi E, Yamazaki K, Nakayama E, Sato S, Uenaka A, Yamada N, et al. Prolonged survival of patients with lung adenocarcinoma expressing XAGE-1b and HLA class I antigens. Cancer Immun 2008;8:13.
21. Ohue Y, Eikawa S, Okazaki N, Mizote Y, Isobe M, Uenaka A, et al. Spontaneous antibody, and CD4 and CD8 T-cell responses against XAGE-1b (GAGED2a) in non-small cell lung cancer patients. Int J Cancer 2012;131:E649–58.
22. Schmidt M, Hellwig B, Hammad S, Othman A, Lohr M, Chen Z, et al. A comprehensive analysis of human gene expression profiles identifies stromal immunoglobulin kappa C as a compatible prognostic marker in human solid tumors. Clin Cancer Res 2012;18:2695–703.
23. McNeil LK, Price L, Britten CM, Jaimes M, Maecker H, Odunsi K, et al. A harmonized approach to intracellular cytokine staining gating: Results from an international multiconsortia proficiency panel conducted by the Cancer Immunotherapy Consortium (CIC/CRI). Cytometry A 2013;83:728–38.
24. Gnjatic S, Old LJ, Chen YT. Autoantibodies against cancer antigens. Methods Mol Biol 2009;520:11–9.
25. Miyara M, Yoshioka Y, Kitoh A, Shima T, Wing K, Niwa A, et al. Functional delineation and differentiation dynamics of human CD4+ T cells expressing the FoxP3 transcription factor. Immunity 2009;30: 899–911.
26. Gong Y, Somwar R, Politi K, Balak M, Chmielecki J, Jiang X, et al. Induction of BIM is essential for apoptosis triggered by EGFR kinase inhibitors in mutant EGFR-dependent lung adenocarcinomas. PLoS Med 2007;4:e294.
27. Cragg MS, Kuroda J, Puthalakath H, Huang DC, Strasser A. Gefitinib-induced killing of NSCLC cell lines expressing mutant EGFR requires BIM and can be enhanced by BH3 mimetics. PLoS Med 2007;4: 1681–89.
28. Deng J, Shimamura T, Perera S, Carlson NE, Cai D, Shapiro GI, et al. Proapoptotic BH3-only BCL-2 family protein BIM connects death signaling from epidermal growth factor receptor inhibition to the mitochondrion. Cancer Res 2007;67:11867–75.
29. Costa DB, Nguyen KS, Cho BC, Sequist LV, Jackman DM, Riely GJ, et al. Effects of erlotinib in EGFR mutated non-small cell lung cancers with resistance to gefitinib. Clin Cancer Res 2008;14: 7060–7.
30. Faber AC, Wong KK, Engelman JA. Differences underlying EGFR and HER2 oncogene addiction. Cell Cycle 2010;9:851–2.
31. Prenzel N, Fischer OM, Streit S, Hart S, Ullrich A. The epidermal growth factor receptor family as a central element for cellular signal transduction and diversification. Endocr Relat Cancer 2001;8:11–31.
32. Yarden Y, Sliwkowski MX. Untangling the ErbB signalling network. Nat Rev Mol Cell Biol 2001;2:127–37.
33. Slichenmyer WJ, Fry DW. Anticancer therapy targeting the erbB family of receptor tyrosine kinases. Semin Oncol 2001;28:67–79.
34. Caballero OL, Cohen T, Gurung S, Chua R, Lee P, Chen YT, et al. Effects of CT-Xp gene knock down in melanoma cell lines. Oncotarget 2013;4:531–41.
35. Yang B, O'Herrin S, Wu J, Reagan-Shaw S, Ma Y, Nihal M, et al. Select cancer testes antigens of the MAGE-A, -B, and -C families are expressed in mast cell lines and promote cell viability *in vitro* and *in vivo*. J Invest Dermatol 2007;127:267–75.
36. Katsura Y, Satta Y. Evolutionary history of the cancer immunity antigen MAGE gene family. PLoS ONE 2011;6:e20365.
37. Gjerstorff MF, Rosner HI, Pedersen CB, Greve KB, Schmidt S, Wilson KL, et al. GAGE cancer-germline antigens are recruited to the nuclear envelope by germ cell-less (GCL). PLoS ONE 2012;7: e45819.
38. Gure AO, Chua R, Williamson B, Gonen M, Ferrera CA, Gnjatic S, et al. Cancer-testis genes are coordinately expressed and are markers of poor outcome in non-small cell lung cancer. Clin Cancer Res 2005;11:8055–62.
39. Jager E, Chen YT, Drijfhout JW, Karbach J, Ringhoffer M, Jager D, et al. Simultaneous humoral and cellular immune response against cancer-testis antigen NY-ESO-1: definition of human histocompatibility leukocyte antigen (HLA)-A2-binding peptide epitopes. J Exp Med 1998;187:265–70.
40. Gnjatic S, Wheeler C, Ebner M, Ritter E, Murray A, Altorki NK, et al. Seromic analysis of antibody responses in non-small cell lung cancer patients and healthy donors using conformational protein arrays. J Immunol Methods 2009;341:50–8.
41. Gnjatic S, Nishikawa H, Jungbluth AA, Gure AO, Ritter G, Jager E, et al. NY-ESO-1: review of an immunogenic tumor antigen. Adv Cancer Res 2006;95:1–30.
42. Ding L, Getz G, Wheeler DA, Mardis ER, McLellan MD, Cibulskis K, et al. Somatic mutations affect key pathways in lung adenocarcinoma. Nature 2008;455:1069–75.
43. Matsushita H, Vesely MD, Koboldt DC, Rickert CG, Uppaluri R, Magrini VJ, et al. Cancer exome analysis reveals a T-cell-dependent mechanism of cancer immunoediting. Nature 2012;482:400–4.
44. Robbins PF, Lu YC, El-Gamil M, Li YF, Gross C, Gartner J, et al. Mining exomic sequencing data to identify mutated antigens recognized by adoptively transferred tumor-reactive T cells. Nat Med 2013;19:747–52.
45. Vogelstein B, Papadopoulos N, Velculescu VE, Zhou S, Diaz LA Jr, Kinzler KW. Cancer genome landscapes. Science 2013;339:1546–58.

Published OnlineFirst August 14, 2014; DOI: 10.1158/1078-0432.CCR-14-0742

AACR American Association for Cancer Research

Clinical Cancer Research

Prolongation of Overall Survival in Advanced Lung Adenocarcinoma Patients with the XAGE1 (GAGED2a) Antibody

Yoshihiro Ohue, Koji Kurose, Yu Mizote, et al.

Clin Cancer Res 2014;20:5052-5063. Published OnlineFirst August 14, 2014.

Clinical & Experimental Immunology
The Journal of Translational Immunology

Clinical and Experimental Immunology ORIGINAL ARTICLE doi:10.1111/cei.12247

Genetic variants of immunoglobulin γ and κ chains influence humoral immunity to the cancer-testis antigen XAGE-1b (GAGED2a) in patients with non-small cell lung cancer

J. P. Pandey,* A. M. Namboodiri,* Y. Ohue,§ M. Oka§ and E. Nakayama†
*Department of Microbiology and Immunology, Medical University of South Carolina, Charleston, SC, USA, §Department of Respiratory Medicine, Kawasaki Medical School, and †Faculty of Health and Welfare, Kawasaki University of Medical Welfare, Kurashiki, Japan

Accepted for publication 30 November 2013
Correspondence: J. P. Pandey, Department of Microbiology and Immunology, Medical University of South Carolina, Charleston, SC 29425-2230, USA.
E-mail: pandeyj@musc.edu

Summary

GM (γ marker) allotypes, genetic variants of immunoglobulin γ chains, have been reported to be associated strongly with susceptibility to lung cancer, but the mechanism(s) underlying this association is not known. One mechanism could involve their contribution to humoral immunity to lung tumour-associated antigens. In this study, we aimed to determine whether particular GM and KM (κ marker) allotypes were associated with antibody responsiveness to XAGE-1b, a highly immunogenic lung tumour-associated cancer-testis antigen. Sera from 89 patients with non-small cell lung cancer (NSCLC) were allotyped for eight GM and two KM determinants and characterized for antibodies to a synthetic XAGE-1b protein. The distribution of various GM phenotypes was significantly different between XAGE-1b antibody-positive and -negative patients ($P = 0{\cdot}023$), as well as in the subgroup of XAGE-1b antigen-positive advanced NSCLC ($P = 0{\cdot}007$). None of the patients with the GM 1,17 21 phenotype was positive for the XAGE-1b antibody. In patients with antigen-positive advanced disease, the prevalence of GM 1,2,17 21 was significantly higher in the antibody-positive group than in those who lacked the XAGE-1b antibody ($P = 0{\cdot}026$). This phenotype also interacted with a particular KM phenotype: subjects with GM 1,2,17 21 and KM 3,3 phenotypes were almost four times (odds ratio = 3·8) as likely to be positive for the XAGE-1b antibody as the subjects who lacked these phenotypes. This is the first report presenting evidence for the involvement of immunoglobulin allotypes in immunity to a cancer-testis antigen, which has important implications for XAGE-1b-based immunotherapeutic interventions in lung adenocarcinoma.

Keywords: cancer-testis antigen, GM/KM allotypes, humoral immunity, non-small cell lung cancer, XAGE-1b (GAGED2a)

Introduction

Genetic variants of immunoglobulin G (IgG) heavy chains are called GM allotypes. They are encoded by three very closely linked genes – immunoglobulin heavy chain G1 (*IGHG1*), *IGHG2* and *IGHG3* – on chromosome 14q32. They are expressed on the constant regions of γ1, γ2 and γ3 chains. There are striking qualitative and quantitative differences in the distribution of GM allotypes among different racial groups. In addition, there is almost complete linkage disequilibrium between particular GM determinants within a race, and every major racial group is characterized by a distinct array of GM haplotypes [1,2]. Using hypothesis-driven candidate gene approaches, several studies have identified particular GM genes/genotypes as risk factors for many malignant diseases [2–7]. In lung cancer, a highly significant association was found between the GM 1,2 13,15,16,21 phenotype and susceptibility to this malignancy in a Japanese population [8]. The mechanism(s) underlying this association is not known.

One mechanism underlying the reported GM gene–lung cancer association could involve the contribution of GM determinants to humoral immunity to lung tumour-associated antigens, as GM genes are known to influence immunity to several self and non-self antigens, including tumour-associated antigens mucin 1 and human epidermal

growth factor receptor 2 [9–14]. In this investigation, we aimed to determine whether GM allotypes are associated with antibody responsiveness to XAGE-1b, a highly immunogenic lung tumour-associated antigen that belongs to the cancer-testis antigen gene families [15–17]. A recent comprehensive analysis of human gene expression has identified the Ig κ constant (*IGKC*) gene as a strong prognostic marker in human solid tumours, including lung cancer [18]. Identification of tumour-infiltrating plasma cells as the source of *IGKC* expression in this study strongly suggests a role for humoral immunity in lung cancer and provides a compelling rationale for investigating the role of KM alleles, genetic variants of *IGKC*, in humoral immunity to lung tumour-associated antigens.

There is increasing evidence that genes do not act in isolation, and that epistasis – modification of the action of a gene by one or more other genes – plays a significant role in human diseases. Genes expressed on the Ig heavy and light chains are probably some of the most likely candidates for gene–gene interactions in the human genome. Therefore, the aim of the present investigation was to determine whether GM and KM allotypes – individually or in particular epistatic combinations – contribute to antibody responsiveness to XAGE-1b in patients with non-small cell lung cancer (NSCLC).

Materials and methods

Blood samples

The study population is described in detail elsewhere [17]. The Institutional Review Boards of the respective institutions approved the study protocol. Blood samples from 89 Japanese patients with NSCLC were included in this investigation. Of these, 80 patients were diagnosed histologically examining available tumour specimens and nine were diagnosed cytologically using tumour cells in pleural effusion, sputum or bronchoalveolar fluid (BALF) because tumour tissue was not available.

Anti-XAGE-1b antibody determinations

These antibodies were measured by a previously described enzyme-linked immunosorbent assay (ELISA) [16,17]. Briefly, synthetic XAGE-1b (GAGED2a) protein (1 μg/ml) in coating buffer was adsorbed onto a 96-well ELISA plate (Nunc, Roskilde, Denmark) and incubated overnight at 4°C. Plates were washed with phosphate-buffered saline (PBS) and blocked with 5% fetal calf serum (FCS)/PBS (200 μl/well) for 1 h at 37°C. After washing, 100 μl of serially diluted serum was added to each well and incubated for 2 h at 4°C; horseradish peroxidase (HRP)-conjugated goat anti-human IgG (MBL) was then added to the wells, and the plates were incubated for 1 h at 37°C. After washing and development, absorbance [optical density (OD)] was read at 490 nm. Sera with OD values exceeding 1·0 at a dilution of 1:300 were considered positive for the XAGE-1b antibody, while those with OD values less than 0·2 were considered negative for this antibody. Patients who showed OD values between 0·2 and 1·0 were excluded. Of the 89 NSCLC patients, 29 were positive for the XAGE-1b antibody and 60 were negative.

Immunohistochemistry

Tumour specimens from 80 patients were also examined by immunohistochemistry. Surgically resected tissues were fixed with buffered formalin and embedded in paraffin. Five-micrometre sections were deparaffinized with xylene and ethanol. Antigen retrieval and inactivation of endogenous peroxidase have been described previously [16]. After incubation with 0·1% Tween 20/5% FCS/PBS for 1 h, the USO 9–13 monoclonal antibody (mAb) was placed at a concentration of 2 μg/ml and incubated for 1 h at room temperature. Immunofluorescence staining was performed as described above. For intracellular localization, rhodamine-conjugated wheat germ agglutinin (WGA) (Vector Laboratories, Burlingame, CA, USA) and 4′,6-diamidino-2-phenylindole (DAPI) (Vector Laboratories) were used. The stained cells were visualized under a digital high-definition microscopic system (model BZ-9000 for the magnification of ×40; Keyence, Osaka, Japan).

Of 80 patients, 46 were XAGE-1b antigen-positive and 34 were antigen-negative. Detailed clinical information was not available for three antigen-positive patients. Of the remaining 43 antigen-positive patients, 26 were antibody-positive and 17 were antibody-negative.

GM and KM allotyping

Serum samples were typed for G1M (1/a, 2/x, 3/f, 17/z), G2M (23/n), G3M (5/b1, 13/b3, 21/g) and KM 1 and 3 allotypes by a standard haemagglutination-inhibition method [19]. In brief, a mixture containing human blood group O rhesus-positive (ORh^+) erythrocytes coated with anti-Rh antibodies of known GM/KM allotypes, the test sera and monospecific anti-allotype antibodies were incubated in a microtitre plate. Test sera containing IgG of the particular allotype inhibited haemagglutination by the anti-allotype antibody, whereas negative sera did not. The notation for GM allotypes follows the international system for human gene nomenclature, in which haplotypes and phenotypes are written by grouping together the markers that belong to each IgG subclass, by the numerical order of the marker and of the subclass; markers belonging to different subclasses are separated by a space, while allotypes within a subclass are separated by commas.

Three alleles – KM 1, KM 1,2 and KM 3 – segregate at the KM locus on chromosome 2p12. More than 98% of people positive for KM 1 are also positive for KM 2. The KM 1

Table 1. Distribution of GM* and KM phenotypes in the XAGE-1b antibody-positive and -negative patients with lung adenocarcinoma ($n = 89$).

	XAGE-1b antibody				
Phenotype	Positive ($n = 29$)	(%)	Negative ($n = 60$)	(%)	*P*-value
GM 1,17 21	0	0	10	16·7	0·027
GM 1,2,17 21	15	51·7	19	31·7	0·06
GM 1,17 13,21	0	0	4	6·7	0·30
GM 1,2,17 13,21	1	3·4	8	13·3	0·26
GM 1,2,3,17 23 5,13,21	2	6·9	5	8·3	1·0
Other GM	11	37·9	14	23·3	0·21
KM 1	3	10·3	6	10·0	0·61
KM 1,3	8	27·6	26	43·3	0·15
KM 3	11	62·1	28	46·7	0·17

*Fisher's exact test (6×2), $P = 0·023$.

allele, without KM 2, is extremely rare. Here, and in most other investigations, positivity for KM 1 includes both KM 1 and KM 1,2 alleles.

Statistical analysis

The significance of the association between GM and KM phenotypes and the prevalence of antibodies to XAGE-1b in NSCLC patients was analysed using Fisher's exact test and Pearson's χ^2 test. Subjects with very unusual GM phenotypes and those whose frequency was <4% were combined as 'other', in order not to have a test with too many degrees of freedom. Associations between the prevalence of antibodies and GM phenotypes and patient survival were assessed using a Cox regression model. Statistical significance was defined as $P < 0·05$. All reported *P*-values are two-sided.

Results

Table 1 presents the distribution of GM and KM phenotypes in XAGE-1b antibody-positive and -negative patients with lung adenocarcinoma. The majority of the subjects possessed typical Japanese GM phenotypes, which can be explained by postulating the segregation of four haplotypes present in this population: GM 1,17 21, GM 1,2,17 21, GM 1,17 13 and GM 1,3 23 5,13. The frequency of KM phenotypes observed was also typical of this population.

A global Fisher's exact test, considering all GM phenotypes, shows that there is a significant difference in the distribution of various phenotypes between the XAGE-1b antibody-positive and -negative groups of patients ($P = 0·023$). Further dissection of this association elucidates that the discrepancy in the distribution of GM 1,17 21 and GM 1,2,17 21 phenotypes contributed most to the total variation. None of the subjects with the GM 1,17 21 phenotype was positive for the XAGE-1b antibody ($P = 0·027$). The frequency of the GM 1,2,17 21 phenotype in the antibody-positive group was higher than in the antibody-negative group, but it did not reach statistical significance (52 *versus* 32%; Pearson's $\chi^2 = 3·3$; $P = 0·06$). However, in subjects who were also homozygous for the KM 3 allele, this GM phenotype contributed significantly to the antibody responsiveness: subjects with GM 1,2,17 21 and KM 3,3 phenotypes were almost four times [odds ratio (OR) = 3·8] as likely to be positive for the XAGE-1b antibody as the subjects who lacked both these phenotypes (Table 2). No other significant interactions were found. Also, none of the KM phenotypes alone was associated with anti-XAGE-1b antibody responsiveness.

Subsequent analyses were restricted to patients with XAGE-1b antigen-positive advanced (IIIB/IV) lung cancer. The clinical and demographic characteristics of these patients are presented in Table 3. The prevalence of anti-XAGE-1b antibodies was higher in patients with less advanced disease ($P = 0·030$). Other characteristics, except age, were not significantly different in the two groups of patients. A global Fisher's exact test, considering all GM phenotypes, shows that there is a significant difference in the distribution of various phenotypes between the XAGE-1b antibody-positive and -negative groups of patients with XAGE-1b antigen-positive advanced lung cancer ($P = 0·007$). There were only three patients with the GM 1,17 21 phenotype in this group, and all were negative for the XAGE-1b ($P = 0·055$, Table 4). The prevalence of GM 1,2,17 21 was significantly higher in the antibody-positive group than in those who lacked the XAGE-1b antibody (54 *versus* 18%; $P = 0·026$). The only allotype different between the responder and non-responder phenotypes is the γ1 determinant GM 2, prompting us to analyse the

Table 2. Distribution of combined GM 1,2,17 21 and KM 3,3 phenotypes in antibody-positive and -negative patients in relation to existence of XAGE-1b antibody ($n = 89$).

	XAGE-1b antibody			
Phenotype	Positive $n = 29$ (%)	Negative $n = 60$ (%)	OR (95% CI)	*P*-value
GM 1,2,17 21(+)/KM 3,3 (+)	11 (37·9)	9 (15·0)	3·8 (1·1–13·1)	0·04
GM 1,2,17 21(+)/KM 3,3 (−)	4 (13·8)	10 (16·7)	1·3 (0·3–5·3)	1·0
GM 1,2,17 21(−)/KM 3,3 (+)	7 (24·1)	19 (31·7)	1·2 (0·3–3·9)	1·0
GM 1,2,17 21(−)/KM 3,3 (−)	7 (24·1)	22 (36·7)	1·0	

CI: confidence interval; OR: odds ratio.

Table 3. Characteristics of the patients with XAGE-1b antigen-positive advanced lung cancer ($n = 43$).

	XAGE-1b antibody		
Characteristic	Positive ($n = 26$)	Negative ($n = 17$)	*P*- value
Sex, no. (%)			
Male/female	13/13 (50·0)	13/4 (76·5)	0·11
Age, years			
Mean	76·5 ± 7·6	69·8 ± 10·1	0·018
Smoking status, no. (%)			
Never smoked	10 (38·5)	5 (29·4)	0·75
ECOG performance status score, no. (%)			
0–1	21 (80·8)	11 (64·7)	0·30
Clinical stage, no. (%)			
IIIB/IV	10/16 (38·5)	1/16 (5·9)	0·030
Brain metastasis, no. (%)			
positive/negative	9/17 (34·6)	5/12 (29·4)	0·75
EGFR mutation, no. (%)			
Positive/negative	13/13 (50·0)	4/13 (23·5)	0·12

ECOG: Eastern Cooperative Oncology Group; EGFR: epidermal growth factor receptor.

interindividual variation in antibody responsiveness in relation to the GM 2 status of the subjects. No significant associations were found in the whole group ($P = 0·34$) as well as in the XAGE-1b antigen-positive group ($P = 0·18$). Thus, it appears that the influence of GM 2 on antibody responsiveness is manifested only when it is in a complex with γ1 determinants GM 1 and 17 and the γ3 determinant GM 21. Although a significant interactive effect of GM 1,2,17 21 with KM 3 homozygosity was observed (OR = 10; $P = 0·04$), this association should be viewed with caution, as the number of subjects in some categories was very small, resulting in a wide confidence interval (data not shown).

Of the 43 patients with antigen-positive tumours, 17 were negative for the XAGE-1b antibody; however, only one of these belonged to the clinical stage IIIB, the rest being clinical stage IV. Therefore, survival curves were plotted with the stage IV patients as well as with the combined group of patients with clinical stages IIIB and IV. As shown in Fig. 1, the anti-XAGE-1b antibody positivity was associated significantly with enhanced overall survival in both groups of patients, the antibody-positive subjects surviving more than twice as long as those who lacked this antibody (stage IIIB/IV: 33 *versus* 14 months, $P = 0·007$; stage IV: 33 *versus* 13 months, $P = 0·039$). Although not statistically significant (due possibly to the small sample size), stage IIIB/IV subjects with the GM 1,2,17 21 phenotype, which was associated with a higher prevalence of anti-XAGE-1b antibodies, survived longer than those expressing the GM 1,17 21 phenotype, which was associated with the lack of antibodies to XAGE-1b (31 *versus* 15 months, $P = 0·29$, Fig. 2).

Discussion

The results presented here show that the Ig GM 1,2,17 21 phenotype is associated with the presence of naturally occurring antibodies to the cancer-testis antigen XAGE-1b, while the GM 1,17 21 phenotype is associated with the lack of such antibodies. One mechanism underlying this association could involve GM allotypes being part of the recognition structures for the immunogenic epitopes of the XAGE-1b protein. Perhaps membrane-bound IgG (mIgG) molecules with GM 1,2,17 21 allotypes are more efficient in the uptake, processing and subsequent presentation of XAGE-1b epitopes to the collaborating T cells, resulting in strong humoral immunity, whereas the mIgG molecules with the GM 1,17 21 phenotype form a lower affinity receptor for the critical epitopes of this protein. Additionally – and contrary to the prevalent belief in immunology – these constant-region determinants could directly influence anti-XAGE-1b antibody specificity by causing conformational changes in the antigen-binding site in the Ig variable region. There is convincing evidence that the Ig constant region can influence antibody affinity and specificity [20]. Thus, constant regions expressing different GM allotypes, even when combined with identical variable region sequences, can generate new antibody molecules with new functions. They could also influence the expression of idiotypes involved in XAGE-1b immunity. The contribution of both variable and constant regions in the formation of idiotypic determinants has been clearly documented for the T15 system in mice, and such isotype-restricted idiotypes have been postulated to be involved in the regulation of class-specific antibody responses [21].

We also found that subjects with GM 1,2,17 21 and KM 3,3 phenotypes were significantly more likely to generate anti-XAGE-1b antibodies than subjects who lacked both these phenotypes. The simultaneous involvement of both GM and KM alleles on antibody responsiveness would

Table 4. Distribution of GM* and KM phenotypes in the XAGE-1b antibody-positive and -negative patients with XAGE-1b antigen-positive advanced lung adenocarcinoma ($n = 43$).

	XAGE-1b antibody				
Phenotype	Positive ($n = 26$)	(%)	Negative ($n = 17$)	(%)	*P*-value
GM 1,17 21	0	0	3	17·6	0·055
GM 1,2,17 21	14	53·8	3	17·6	0·026
GM 1,17 13,21	0	0	1	5·9	0·40
GM 1,2,17 13,21	1	3·8	4	23·5	0·07
GM 1,2,3,17 23 5,13,21	1	3·8	1	5·9	1·0
Other GM	10	38·5	5	29·4	0·75
KM 1	3	11·5	2	11·7	1·0
KM 1,3	8	30·8	7	41·2	0·53
KM 3	15	57·7	8	47·1	0·55

*Fisher's exact test (6×2), $P = 0·007$.

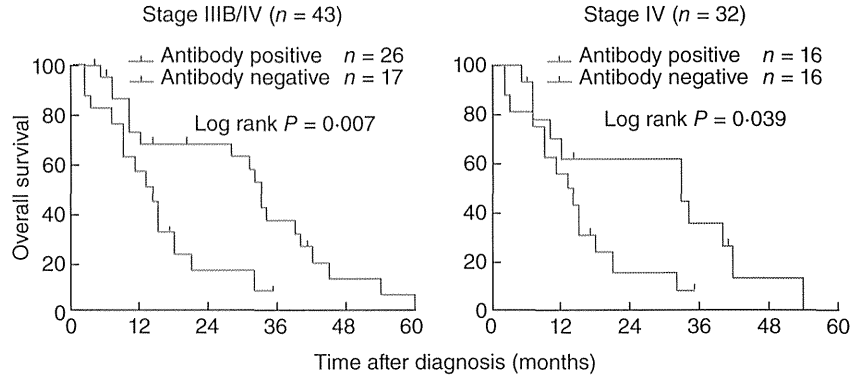

Stage	Overall survival	Antibody		*P*-value
		Positive	Negative	
Stage IIIB/IV	Median, month	33·0	14·0	0·007
	95% CI	30·3–35·7	8·2–19·8	
Stage IV	Median, month	33·0	13·0	0·039
	95% CI	0–66·1	7·1–18·9	

Fig. 1. Kaplan–Meier survival plots of XAGE-1b antigen-positive advanced lung adenocarcinoma patients as a function of XAGE-1b antibody.

suggest that the association of γ and κ chains in IgG antibodies directed against XAGE-1b might not be random. Only γ and κ chains carrying specific GM and KM allotypes might form a paratope with the necessary quaternary structure for an effective recognition of the XAGE-1b epitopes. Non-random pairing of heavy and light chains has been reported in experimental animals [22,23].

As mentioned previously, the XAGE-1b antigen is highly immunogenic and, therefore, an excellent vaccine candidate for active immunotherapy. In XAGE-1b antibody-positive patients, specific T cell responses were also frequently observed [17]. If the results presented here are confirmed in an independent study, they could aid in identifying subjects (GM 1,2,17 21) who are more likely to benefit from XAGE-1b-based vaccines. For those with the non-responder (GM 1,17 21) phenotype, XAGE-1b could be fused with appropriate adjuvants, such as heat shock proteins or flagellin, to overcome the allotypic restriction in immune responsiveness. It is relevant to note that antibody responses to certain heat shock proteins as well as to flagellin are also influenced by GM genotypes [24,25], making it conceivable to formulate a fusion XAGE-1b–heat shock protein/flagellin vaccine that could potentially generate high antibody responses in the majority of the population. Identification of the natural responders/non-responders to XAGE-1b would also be helpful in the proper evaluation of any future vaccine efficacy trials.

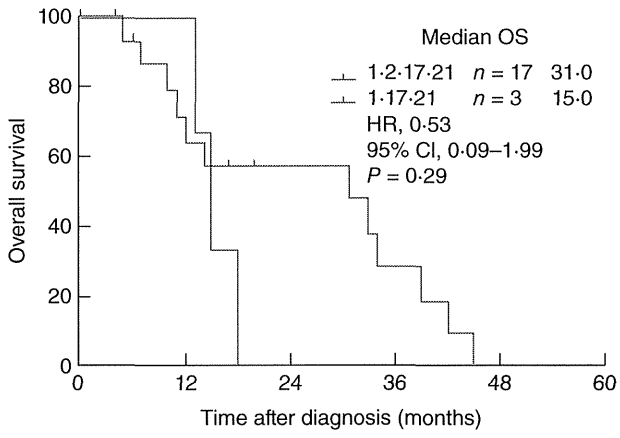

Fig. 2. Kaplan–Meier survival plots of XAGE-1b antigen-positive stage IIIB/IV lung adenocarcinoma patients as a function of GM 1,2,17 21 and GM 1,17 21 phenotypes.

Associations observed in this report can also be explained by postulating as-yet unidentified immune response genes for XAGE-1b whose alleles might be in linkage disequilibrium with those of GM and KM loci.

Although the results reported here are statistically significant, they could also be the result of chance fluctuations, as the *P*-values for the associations were not adjusted for multiple testing. Such adjustment is controversial [26], and in the present investigation would be overly punitive, as the multiple tests performed are not independent due to significant linkage disequilibrium in the GM gene complex. This is the first study of its kind, and needs to be replicated and extended by independent investigations.

It is relevant to point out that the highly significant GM phenotype–lung cancer association that was reported more than three decades ago [8] has not been confirmed or refuted by modern genome-wide association studies (GWAS) of this malignancy [27]. One contributing factor for this omission might be the absence of GM gene probes in most genotyping platforms. GWAS are assumed to be able to detect/tag all single nucleotide polymorphisms (SNPs) in the genome whose frequency is at least 5%. This, however, is not true. Most GM alleles are common within a racial group (some with allele frequency >70%), but the *IGHG* gene segments harbouring them are highly homologous and apparently not amenable to the high-throughput genotyping technology used in GWAS. Because these genes

were not typed in the HapMap or the 1000 Genomes projects, they cannot be imputed or tagged (through linkage disequilibrium) by any SNPs that are included in the genotyping platforms. Therefore, a candidate gene approach would be necessary to confirm/refute the findings reported here.

It is hoped that these results, coupled with those identifying the *IGKC* gene as a strong prognostic marker in human solid tumours [18], would inspire large-scale studies to determine conclusively the contribution of Ig GM and KM alleles in humoral immunity to XAGE-1b. It would also be of interest to investigate the role of these determinants in immunity to NY-ESO-1, a prototype cancer-testis antigen. Results from such investigations would be extremely valuable in devising novel immunotherapeutic interventions in patients with lung adenocarcinoma.

Acknowledgements

The study was supported by Project for Development of Innovative Research on Cancer Therapeutics of Ministry of Education, Culture Sports Science and Technology of Japan.

Disclosure

The authors have no conflicts of interest to declare.

References

1 Grubb R. Advances in human immunoglobulin allotypes. Exp Clin Immunogenet 1995; **12**:191–7.
2 Pandey JP, Li Z. The forgotten tale of immunoglobulin allotypes in cancer risk and treatment. Exp Hematol Oncol 2013; **2**:6.
3 Pandey JP, Kistner-Griffin E, Iwasaki M *et al.* Genetic markers of immunoglobulin G and susceptibility to breast cancer. Hum Immunol 2012; **73**:1155–8.
4 Morell A, Scherz R, Käser H, Skvaril F. Evidence for an association between uncommon Gm phenotypes and neuroblastoma. Lancet 1977; **1**:23–4.
5 Ilić V, Milosević-Jovcić N, Marković D *et al.* A biased Gm haplotype and Gm paraprotein allotype in multiple myeloma suggests a role for the Gm system in myeloma development. Int J Immunogenet 2007; **34**:119–25.
6 Pandey JP, Johnson AH, Fudenberg HH *et al.* HLA antigens and immunoglobulin allotypes in patients with malignant melanoma. Hum Immunol 1981; **2**:185–90.
7 Pandey JP, Ebbesen P, Bülow S *et al.* IgG heavy-chain (Gm) allotypes in familial polyposis coli. Am J Hum Genet 1986; **39**:133–6.
8 Nakao Y, Matsumoto H, Miyazaki T *et al.* Immunoglobulin G heavy-chain allotypes as possible genetic markers for human cancer. J Natl Cancer Inst 1981; **67**:47–50.
9 Pandey JP, Namboodiri AM, Kistner-Griffin E. IgG and FcγR genotypes and humoral immunity to mucin 1 in prostate cancer. Hum Immunol 2013; **74**:1030–33.
10 Pandey JP, Nietert PJ, Mensdorff-Pouilly S *et al.* Immunoglobulin allotypes influence antibody responses to mucin 1 in patients with gastric cancer. Cancer Res 2008; **68**:4442–46.
11 Pandey JP, Nietert PJ, Klaamas K *et al.* A genetic variant of immunoglobulin γ2 is strongly associated with natural immunity to mucin 1 in patients with breast cancer. Cancer Immunol Immunother 2009; **58**:2025–29.
12 Pandey JP, Namboodiri AM, Kurtenkov O *et al.* Genetic regulation of antibody responses to human epidermal growth factor receptor 2 (HER-2) in breast cancer. Hum Immunol 2010; **71**:1124–27.
13 Pandey JP, Namboodiri AM, Kistner-Griffin E *et al.* Racially restricted contribution of immunoglobulin Fcγ and Fcγ receptor genotypes to humoral immunity to human epidermal growth factor receptor 2 in breast cancer. Clin Exp Immunol 2013; **171**:273–7.
14 Pandey JP, Shannon BT, Tsang KY *et al.* Heterozygosity at Gm loci associated with humoral immunity to osteosarcoma. J Exp Med 1982; **155**:1228–32.
15 Ali Eldib AM, Ono T, Shimono M *et al.* Immunoscreening of a cDNA library from a lung cancer cell line using autologous patient serum: identification of XAGE-1b as a dominant antigen and its immunogenicity in lung adenocarcinoma. Int J Cancer 2004; **108**:558–63.
16 Nakagawa K, Noguchi Y, Uenaka A *et al.* XAGE-1 expression in non-small cell lung cancer and antibody response in patients. Clin Cancer Res 2005; **11**:5496–503.
17 Ohue Y, Eikawa S, Okazaki N *et al.* Spontaneous antibody, and CD4 and CD8 T-cell responses against XAGE-1b (GAGED2a) in non-small cell lung cancer patients. Int J Cancer 2012; **131**:E649–58.
18 Schmidt M, Hellwig B, Hammad S *et al.* A comprehensive analysis of human gene expression profiles identifies stromal immunoglobulin kappa C as a compatible prognostic marker in human solid tumors. Clin Cancer Res 2012; **18**:2695–704.
19 Schanfield MS, van Loghem E. Human immunoglobulin allotypes. In: Weir DM, ed. Handbook of experimental immunology. Boston, MA: Blackwell, 1986:94.1–18.
20 Casadevall A, Pirofski L-A. A new synthesis for antibody-mediated immunity. Nat Immunol 2012; **13**:21–8.
21 Morahan G, Berek C, Miller JFAP. An idiotypic determinant formed by both immunoglobulin constant and variable regions. Nature 1983; **301**:720–22.
22 Czerwinski M, Siemaszko D, Siegel DL *et al.* Only selected light chains combine with a given heavy chain to confer specificity for a model glycopeptide antigen. J Immunol 1998; **160**:4406–17.
23 Primi D, Drapier AM, Cazenave PA. Highly preferential VH–VL pairing in normal B cells results in antigen-independent selection of the available repertoire. J Immunol 1987; **138**:1607–12.
24 Pandey JP, Prohászka Z, Veres A *et al.* Epistatic effects of genes encoding immunoglobulin GM allotypes and interleukin-6 on the production of autoantibodies to 60- and 65-kDa heat-shock proteins. Genes Immun 2004; **5**:68–71.
25 Pandey JP. Comment on 'Flagellin as an adjuvant: cellular mechanisms and potential'. J Immunol 2011; **186**:1299.
26 Perneger TV. What's wrong with Bonferroni adjustments. BMJ 1998; **316**:1236–38.
27 Shiraishi K, Kunitoh H, Daigo Y *et al.* A genome-wide association study identifies two new susceptibility loci for lung adenocarcinoma in the Japanese population. Nat Genet 2012; **44**:900–3.

Published online 27 September 2014

Nucleic Acids Research, 2014, Vol. 42, No. 19 ***11903–11911***
doi: 10.1093/nar/gku881

HSP90α plays an important role in piRNA biogenesis and retrotransposon repression in mouse

Tomoko Ichiyanagi[1,2,†], Kenji Ichiyanagi[2,†], Ayako Ogawa[2], Satomi Kuramochi-Miyagawa[3,4], Toru Nakano[3,4], Shinichiro Chuma[5], Hiroyuki Sasaki[2] and Heiichiro Udono[1,*]

[1]Department of Immunology, Okayama University Graduate School of Medicine, Dentistry, and Pharmaceutical Sciences, Kita-ku, Okayama 700-8558, Japan, [2]Division of Epigenomics and Development, Medical Institute of Bioregulation, Kyushu University, Higashi-ku, Fukuoka 812-8582, Japan, [3]Department of Pathology, Medical School and Graduate School of Frontier Biosciences, Osaka University, Suita, Osaka 565-0871, Japan, [4]CREST, Japan Science and Technology Agency (JST), Saitama 332-0012, Japan and [5]Department of Development and Differentiation, Institute for Frontier Medical Sciences, Kyoto University, Sakyo-ku, Kyoto 606-8507, Japan

Received July 8, 2014; Revised September 07, 2014; Accepted September 13, 2014

ABSTRACT

HSP90, found in all kingdoms of life, is a major chaperone protein regulating many client proteins. We demonstrated that HSP90α, one of two paralogs duplicated in vertebrates, plays an important role in the biogenesis of fetal PIWI-interacting RNAs (piRNA), which act against the transposon activities, in mouse male germ cells. The knockout mutation of *Hsp90α* resulted in a large reduction in the expression of primary and secondary piRNAs and mislocalization of MIWI2, a PIWI homolog. Whereas the mutation in *Fkbp6* encoding a co-chaperone reduced piRNAs of 28–32 nucleotides in length, the *Hsp90α* mutation reduced piRNAs of 24–32 nucleotides, suggesting the presence of both FKBP6-dependent and -independent actions of HSP90α. Although DNA methylation and mRNA levels of L1 retrotransposon were largely unchanged in the *Hsp90α* mutant testes, the L1-encoded protein was increased, suggesting the presence of post-transcriptional regulation. This study revealed the specialized function of the HSP90α isofom in the piRNA biogenesis and repression of retrotransposons during the development of male germ cells in mammals.

INTRODUCTION

Heat-shock protein 90 (HSP90), the most abundant protein in mammalian cells, is a chaperone that stabilizes the conformation of >200 client proteins in various physiological pathways, thereby maintaining cellular homeostasis (1,2). In mammals, there are two cytosolic HSP90 isoforms encoded by distinct genes, *Hsp90aa1* (HSP86; HSP90α) and *Hsp90ab1* (HSP84; HSP90β) sharing 86% similarity in amino acid sequences, as well as HSP90 family proteins localized in the mitochondria and endoplasmic reticulum. For simplicity, we refer to *Hsp90aa1* and *Hsp90ab1* as *Hsp90α* and *Hsp90β*, respectively. Although *Hsp90β* is ubiquitously expressed (constitutive type), *Hsp90α* expression is increased in response to various stresses (inducible type), and its expression is more tissue-specific at the steady state, being relatively higher in the testes and brain (3–5). Whether these HSP90 proteins have specific functions remains unclear.

Recently, plant and insect HSP90 proteins were implicated in the biogenesis of three major classes of small RNAs: small interfering RNA (siRNA), microRNA (miRNA) and PIWI-interacting RNA (piRNA). In insects and plants, the ATPase activities of HSP90 and HSP70 are indispensable for the formation of the pre-RNA-induced silencing complex (pre-RISC), in which double-stranded RNA precursors of siRNA and miRNA are loaded onto Argonaute proteins (6–8). In cultured human cells, however, chemical inhibition of HSP90 proteins does not affect miRNA expression, although Argonaute-2 is mislocalized (9). In animal gonads, PIWI-clade Argonaute proteins (Piwi, Aub and Ago3 in flies and MILI, MIWI and MIWI2 in mice) play a principal role in the generation of piRNAs, germline-specific small RNAs typically 24–33 nucleotides (nt) in length that counteract the transposon activities (10). In flies, Hsp90 has been implicated in piRNA production (11,12), and its co-chaperone, Hop, regulates Piwi phosphorylation and thus piRNA production (12). Moreover, silkworm Hsp90 participates in the loading of piRNA precursors onto Piwi (13). Another Hsp90 co-chaperone, Shutdown, is important for piRNA production in flies (14), and its mouse ortholog, FKBP6, has been proposed to facilitate the recycling of PIWI proteins in piRNA biogenesis

*To whom correspondence should be addressed. Tel: +81 86 235 7187; Fax: +81 86 235 7193; Email: udono@cc.okayama-u.ac.jp
†The authors wish it to be known that, in their opinion, the first two authors should be regarded as Joint First Authors.

(15). However, whether HSP90 plays a role in piRNA biogenesis in mice and other vertebrate species remains unknown. Studies on the role of the mouse HSP90 proteins in piRNA biogenesis have been hindered by the presence of two *Hsp90* genes in mice versus a single gene in insects. *Hsp90α* knockout (KO) mice are viable, presumably because of the presence of functional *Hsp90β*. However, we revealed that KO males are infertile due to a failure in spermatogenesis (16,17), suggesting that *Hsp90α* plays a role in spermatogenesis that cannot be replaced by *Hsp90β*. In this study, we investigated piRNA biogenesis in *Hsp90α* KO mice and revealed a specific function of HSP90α in the piRNA-based host-defense system against transposons in mice.

MATERIALS AND METHODS

Animals

The *Hsp90α* and *Mitopld* KO strains were described by Kajiwara *et al.* (17) and Watanabe *et al.* (18), respectively.

Antibodies

Polyclonal antibodies to HSP86 (HSP90α) and HSP84 (HSP90β) were purchased from Thermo Scientific (PA3–013, RB-118). For immunostaining, polyclonal antibodies against MILI (PIWIL2), MIWI2 (PIWIL4) and WDR77 were purchased from Abcam. Anti-TDRD1 and TDRD9 polyclonal antibodies and anti-MIWI2 polyclonal antibody for immunoprecipitation were made by S. C. (Kyoto University) and S. K.-M. (Osaka University), respectively. Anti-L1 ORF polyclonal antibody and *Mael* KO testes lysate were generous gifts from Dr A. Bortvin (Carnegie Institute) (19). Anti-mono and dimethyl arginine monoclonal antibody (7E6) used in western blot analysis was obtained from Abcam.

Oligonucleotides

The sequences of oligonucleotides used in this study are listed in Supplementary Table S1.

Immunofluorescence detection of protein localization

E16.5–18.5 testes were embedded in OCT compound and snap-frozen in liquid nitrogen or isopentane cooled in liquid nitrogen. Cryosections were cut at 7–10-μm thickness and air-dried. The sections were fixed for 10 min in 4% PFA at 4°C, washed with PBS, permeabilized in PBS with 0.5% Triton X-100 for 30 min at room temperature, and blocked in PBS with 0.1% Triton X-100 and 1% BSA for 30 min at room temperature. Primary antibodies were incubated overnight at 4°C. Slides were washed and incubated with Alexa Fluor 488-labeled secondary antibody for 2–3 h at room temperature. The sections were mounted with SlowFade Gold Antifade Reagent with DAPI (Life Technologies) and observed by fluorescence microscopy.

Small RNA sequencing analysis

Total RNA was extracted from wild-type (WT) and *Hsp90α* KO testes on E16.5 (20 testes for each condition) by Isogen (Toyobo, Japan) and used to create a small RNA library using the TruSeq Small RNA Library Preparation Kit (Illumina). The libraries were sequenced on MiSeq (Illumina) via 50-bp single-end sequencing. After clipping the adaptor sequence, sequence reads of more than 10 bp were mapped to cellular RNA and miRNA sequences in miRBase (20) by SeqMap (21). Unmapped sequences were then mapped to the mouse genome sequence, allowing no mismatch, and the mouse transposon sequences obtained from RepBase (22), allowing 2-bp mismatches. For piRNA cluster-derived RNAs, the sequences uniquely mapped to the fetal piRNA clusters (23) were analyzed.

The small RNA sequencing data were obtained from Gene Expression Omnibus (GEO) for *Fkbp6* KO and its WT control (GSE39203). These data and our published data for *Mili* KO, *Miwi2* KO and their WT control (GSE20327) were analyzed using the aforementioned reference sequences.

Immunoprecipitation and western blotting

Three pairs of E16.5 testes were lysed in lysis buffer [20 mM HEPES pH 7.5, 150 mM NaCl, 2.5 mM $MgCl_2$, 0.1% Nonidet P-40 (NP40), 1 mM DTT, protease inhibitor cocktail (Nacalai, Japan)] on ice using a Dounce homogenizer, and the lysate was cleared by centrifugation at 17,800 × g for 15 min at 4°C. The lysate was incubated with anti-MIWI2 antibody overnight at 4°C, following which Protein A/G PLUS-Agarose was added to collect the antibody and protein complexes. The agarose beads were washed four times with wash buffer (25 mM Tris-HCl pH 7.5, 150 mM NaCl, 2.5 mM $MgCl_2$, 0.05% NP40 supplemented with 1 mM DTT, protease inhibitor cocktail). Immunoprecipitants were eluted in sodium dodecyl sulphate (SDS) sample buffer and run on an SDS-polyacrylamide gel electrophoresis gel. Western blotting was performed as described previously (24).

Methylation-sensitive Southern blotting

The genomic DNAs of WT or *Hsp90α* KO testes at P14 (5 μg each) were digested by MspI (methylation insensitive) or HpaII (methylation sensitive) and run on a 0.8% agarose gel. DNAs were then transferred to a Hybond XL membrane (GE Healthcare), hybridized with a ^{32}P-labeled L1 probe (25) at 42°C for 20 h and washed four times with wash buffer (2× SSC, 0.1% SDS) at 42°C. The radioactivities on the membrane were detected on a BAS2500 analyzer (Fujifilm, Japan).

Northern blotting

Total RNA (10 μg each) was run on a 15% polyacrylamide gel, transferred to a Hybond XL membrane using a semi-dry method (100 mA, 2 h) and cross-linked by UV. The membrane was hybridized against radioactive probes at 40°C overnight and washed four times in wash buffer (2× SSC, 0.1% SDS). The L1 (piR-1831) and Intracisternal A particle (IAP) (piR-4868) probes used were described previously (25).

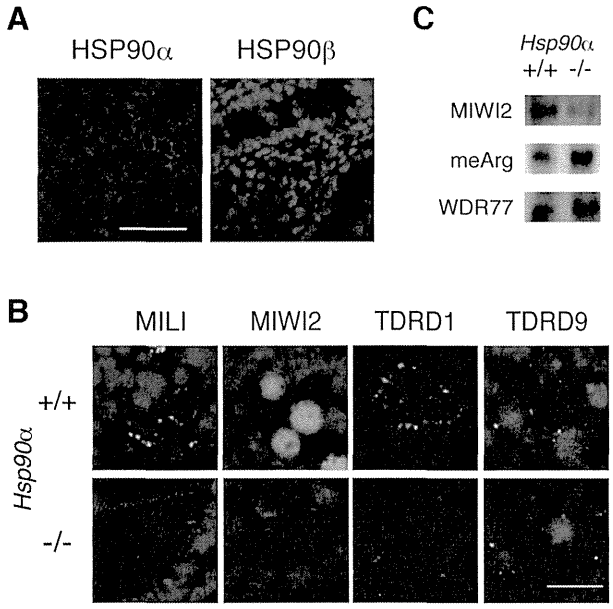

Figure 1. The *Hsp90α* mutation affected the localization but not the arginine methylation of MIWI2. (**A**) Immunofluorescence staining of HSP90α (green; left) or HSP90β (green; right) in WT E18.5 testes. Nuclei were counter-stained with DAPI (blue). (**B**) Localization of piRNA-related proteins (green) in E18.5 WT (top) and Hsp90α KO (bottom) testis. Bars: *A*: 50 μm *B*: 20 μm. (**C**) MIWI2 was immunoprecipitated from the E16.5 testes of WT or Hsp90α KO mice and subjected to western blotting. Immunoprecipitants were blotted for MIWI2 (top), methyl-arginine (middle) and WDR77 (bottom). See also Supplementary Figure S1.

Germ cell preparation and bisulfite sequencing

Germ cells were purified by fluorescence activated cell sorting. Prospermatogonia were isolated from P0 testes of mice carrying an Oct4-EGFP transgene. Spermatocytes were isolated from P17 testes as described previously (26). Genomic DNA was isolated by standard procedure and used for bisulfite sequencing as described previously (27). For each germ cell preparation, the cell purity was validated by confirming the percentages of DNA methylation in the Lit1 differentially methylated region, which is completely unmethylated in male germ cells and 50% methylated in somatic cells.

RESULTS

Hsp90α mutation affects the localization of MIWI2, a PIWI protein

Immunofluorescence analysis revealed that HSP90α is specifically expressed in germ cells (prospermatogonia) in the testis on embryonic day 16.5 (E16.5), whereas HSP90β is expressed in both somatic and germ cells, suggesting a germ cell-specific function of HSP90α (Figure 1A). The prospermatogonia produce piRNAs at this developmental stage, and a deficiency in the biogenesis of fetal piRNAs in animals with mutations in piRNA-related genes such as *Mili*, *Miwi2*, *Tdrd1*, *Tdrd9*, *Mov10l1*, *Maelstrom* and *Mitopld* leads to a failure in spermatogenesis (10). We therefore investigated whether subcellular localization and/or expression levels of piRNA-related proteins are affected by the *Hsp90α* KO mutation in E18.5 testes. Proteins involved in piRNA biogenesis co-localize at granules around the periphery of the nucleus. MILI, one of the two PIWI proteins expressed in prospermatogonia, and TDRD1 localize at cytoplasmic granules at the periphery of nucleus, called pi-bodies, whereas the other PIWI protein MIWI2 as well as TDRD9 and MAELSTROM localizes at different cytoplasmic granules around the nucleus, called piP-bodies (28). MIWI2 and TDRD9 also localize in the nucleus, which is thought to be important for piRNA-targeted DNA methylation (25,29). In *Hsp90α* KO mice, MILI expression and localization were unaffected (Figure 1B and Supplementary Figure S1A). However, we detected an obvious difference in MIWI2 localization. Although MIWI2 localizes both at perinuclear granules and in the nucleus in the WT germ cells, nuclear staining was significantly decreased in *Hsp90α* KO germ cells (Figure 1B), although some staining still remained in nuclei. At the mRNA level, the *Miwi2* expression was not affected in *Hsp90α* KO testes at E16.5 (Supplementary Figure S1B).

Because MIWI2 interacts with TDRD9, a Tudor domain-containing protein (25,30), we investigated TDRD9 expression in *Hsp90α* KO mice as well as the expression of another Tudor protein, TDRD1, which interacts with MILI. The localization of TDRD9 and TDRD1 was unchanged in *Hsp90α* KO mice (Figure 1B). The expression and localization of the other proteins involved in fetal piRNA biogenesis, MAELSTROM and MOV10L1, were also unaffected in *Hsp90α* KO mice (Supplementary Figure S1C).

MIWI2 was methylated at arginines in WT and *Hsp90α* KO testes

The Tudor domains in various proteins specifically bind to methylated arginine residues (31), and it has been postulated that the MIWI2-TDRD9 interaction depends on the methylation of arginine residue(s) in MIWI2 at its RA/RG motifs, which is likely catalyzed by an arginine methyltransferase, PRMT5 (32,33). PRMT5 is a client protein of HSP90, and PRMT5 and HSP90α were found to interact with MIWI2 (32). Moreover, chemical inhibition of HSP90 activity severely diminishes the stability of the PRMT5 protein in cultured cells (34). Therefore, we investigated the arginine methylation of MIWI2 in WT and *Hsp90α* KO mice. For this purpose, MIWI2 was first immunoprecipitated in whole cell lysates of E16.5 testes, and the precipitants were analyzed by western blotting against an anti-methylarginine antibody. We detected an arginine-methylated protein in the WT preparation that co-migrated with MIWI2 in the gel (Figure 1C), suggesting that MIWI2 is indeed methylated at arginine(s) in prospermatogonia. The level of arginine methylation was comparable between WT and KO preparations, suggesting that the arginine methylation of MIWI2 is not disturbed in *Hsp90α* KO mice. Presumably, HSP90β may facilitate PRMT5 activity. WDR77, a co-factor of PRMT5, was detected in the MIWI2-IP fraction of *Hsp90α* KO testes, and the amount was similar to that of WT testes (Figure 1C).

Our results together suggest that in the absence of HSP90α, MIWI2 fails to enter the nucleus even though MIWI2 is methylated and its associated partners, TDRD9

and MAELSTROM, are properly expressed and localized. Failure in MIWI2 translocation is also observed in *Mili*, *Tdrd1*, *Tdrd12*, *Maelstrom*, *Mov10l1* and *Fkbp6* mutant mice (15,25,35–37), all of which are deficient in piRNA biogenesis to various degrees. Therefore, we analyzed small RNAs from WT and *Hsp90α* mutant testes. For comparison, we also analyzed published small RNA sequencing data for *Mili*, *Miwi2* and *Fkbp6* KO testes and their WT controls.

Hsp90α mutation displayed a remarkable decrease in fetal piRNAs

Fetal piRNAs are classified into two types: primary and secondary piRNAs. Primary piRNAs are generated from precursor RNAs transcribed from ~200 genomic regions called piRNA clusters. Transposon-derived RNAs are also the sources of the primary piRNAs. These primary piRNAs preferentially have uracil at the first position, and they are loaded onto MILI. MILI cleaves RNAs containing transposon sequences that are complementary to the primary piRNA. This generates secondary piRNAs, which preferentially have adenine at the 10th position. The secondary piRNAs are loaded onto either MILI or MIWI2 to guide the cleavage of complementary RNAs, a process called the ping-pong cycle. We therefore analyzed both types of piRNAs as well as miRNAs.

Small RNA libraries were generated from WT and *Hsp90α* KO testes at E16.5 and deeply sequenced (Figure 2A). The miRNA reads in the WT and KO libraries were comparable (83.2 and 83.9% of the total 20–23-nt RNAs, respectively). In contrast, the levels of 24–33-nt small RNAs uniquely mapped to the previously identified fetal piRNA clusters, representing primary piRNAs, were reduced by ~3-fold in the KO testes (Figure 2B and C). The levels of 24–33-nt small RNAs mapped to transposon sequences, consisting of primary and secondary piRNAs, were also reduced by ~3-fold (Figure 2D and E). Similar trends were observed in the *Fkbp6* co-chaperone mutant (Figure 2B and D; Xiol *et al.* (15)); however, the effect was larger in *Hsp90α* mutants than in *Fkbp6* mutants. The *Fkbp6* mutation reduced the expression of small RNAs in the range of 28–32 nt, the size range of MIWI2-bound piRNAs; however, it did not affect 24–27-nt RNAs, the size range of MILI-bound piRNAs (Supplementary Figure S2A). In contrast, the *Hsp90α* mutation equally suppressed the expression of 24–32-nt RNAs (Supplementary Figure S2C), suggesting the presence of both FKBP6-dependent and FKBP6-independent actions of HSP90α. In any event, these results indicate that HSP90α plays a role in the biogenesis and/or stability of piRNAs in prospermatogonia. Whereas the *Mili* mutation severely downregulates both cluster- and transposon-derived piRNAs, the *Miwi2* mutation does not reduce cluster-derived piRNAs (Figure 2B and D; Aravin *et al.* (35)). Therefore, the downregulation of both types of piRNAs in *Hsp90α* KO germ cells suggests that HSP90α affects both the activity of MIWI2 and the upstream reaction(s) in the piRNA biogenesis pathway, possibly primary piRNA biogenesis and/or stability.

To study the role of HSP90α in the piRNA pathway in more detail, we analyzed small RNAs mapped to the con-

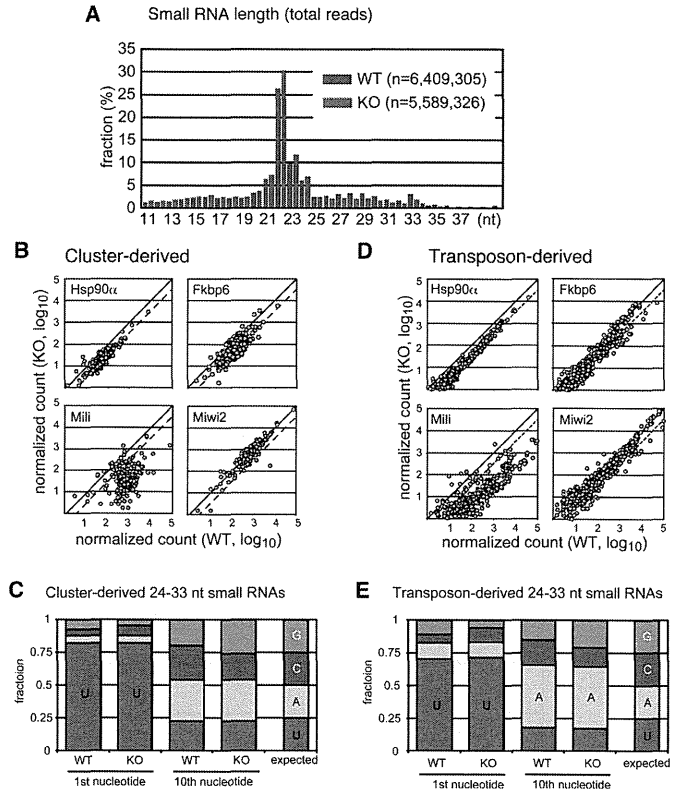

Figure 2. The *Hsp90α* KO mutation reduced both cluster- and transposon-derived small RNAs in E16.5 testes. (**A**) Length distributions of small RNA sequences in WT (blue) and *Hsp90α* KO (red) fetal testes. (**B**, **D**) Small RNA sequence reads (24–33 nt) from *Hsp90α*, *Fkbp6*, *Mili* and *Miwi2* KO testes (vertical axis), which were uniquely mapped to the fetal piRNA clusters (B) or the consensus sequences of mouse transposons (D), are plotted against those from the respective WT controls (horizontal axis). Each plot represents one of the clusters (B) or transposons (D). All sequence reads are normalized as *per million miRNA reads*. The dashed line indicates a 3-fold reduction in the KO library, and the solid line indicates no change. (**C**, **E**) The nucleotide bias at the 1st and 10th positions in the 24–33-nt small RNAs mapped to the piRNA clusters (C) and transposons (E) in WT and KO testes.

sensus sequence of A-type LINE-1 (L1), one of the most active retrotransposons in the mouse genome (Figure 3A). Both sense and antisense small RNA levels were reduced in the KO testes. Although this global reduction, the mapped 24–33-nt small RNAs in the KO library displayed a bias toward uracil at the first position and adenine at the 10th position as well as a 10-bp overlap between sense and antisense small RNAs (Figures 2C, E and 3B), which are the hallmarks of piRNAs generated via the ping-pong cycle. We also detected an ~3-fold reduction in the expression of piRNAs derived from Gf-type L1, another active L1 subfamily, in KO testes.

In addition to the length range of typical piRNAs, we detected a number of 19-nt small RNAs, which were positioned immediately upstream of 24–33-nt piRNAs on the same strand and were complementary to 29-nt piRNAs on the opposite strand (Figure 3A, C, and Supplementary Figure S2). Most (79%) 19-nt RNAs were associated with piRNAs that have adenine at the 10th position, and the 19-nt peak was not observed for cluster-derived small RNAs (Fig-